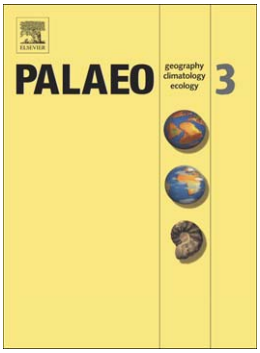

Atlantic Water advection to the eastern Fram Strait – multiproxy evidence for late Holocene variability

Kirstin Werner, Robert F. Spielhagen, Dorothea Bauch, H. Christian Hass, Evgeniya Kandiano, Katarzyna Zamelczyk

PII: S0031-0182(11)00275-6
DOI: doi: 10.1016/j.palaeo.2011.05.030
Reference: PALAEO 5811

To appear in: *Palaeogeography*

Received date: 7 February 2011
Revised date: 2 May 2011
Accepted date: 16 May 2011

Please cite this article as: Werner, Kirstin, Spielhagen, Robert F., Bauch, Dorothea, Hass, H. Christian, Kandiano, Evgeniya, Zamelczyk, Katarzyna, Atlantic Water advection to the eastern Fram Strait – multiproxy evidence for late Holocene variability, *Palaeogeography* (2011), doi: 10.1016/j.palaeo.2011.05.030

Atlantic Water advection to the eastern Fram Strait – multiproxy evidence for late Holocene variability

Kirstin Werner[a,*], Robert F. Spielhagen[a,b], Dorothea Bauch[a,b], H. Christian Hass[c], Evgeniya Kandiano[a] and Katarzyna Zamelczyk[d]

[a] Leibniz Institute of Marine Sciences IFM-GEOMAR, Wischhofstraße 1-3, 24148 Kiel, Germany

[b] Academy of Sciences, Humanities, and Literature Mainz, Geschwister-Scholl-Straße 2, 55131 Mainz, Germany

[c] Alfred Wegener Institute for Polar and Marine Research, Wadden Sea Station Sylt, Hafenstraße 43, 25992 List/Sylt, Germany

[d] University of Tromsø, Department of Geology, Dramsveien 201, NO-9037 Tromsø, Norway

*Corresponding author. Tel.: +49 600 2888; fax: +49 600 2961.

E-mail addresses: kwerner@ifm-geomar.de (K. Werner), rspielhagen@ifm-geomar.de (R. F. Spielhagen), dbauch@ifm-geomar.de (D. Bauch), christian.hass@awi.de (H. C. Hass), ekandiano@ifm-geomar.de (E. Kandiano), katarzyna.zamelczyk@uit.no (K. Zamelczyk)

Abstract: A multiproxy data set of an AMS radiocarbon dated 46 cm long sediment core from the continental margin off western Svalbard reveals multidecadal climatic variability during the past two millennia. Investigation of planktic and benthic stable isotopes, planktic foraminiferal fauna, and lithogenic parameters aims to unveil the Atlantic Water advection to the eastern Fram Strait by intensity, temperatures, and salinities. Atlantic Water has been continuously present at the site over the last 2,000 years. Superimposed on the increase in sea

ice/icebergs, a strengthened intensity of Atlantic Water inflow and seasonal ice-free conditions were detected at ~1000 to 1200 AD, during the well-known Medieval Climate Anomaly (MCA). However, temperatures of the MCA never exceeded those of the 20th century. Since ~1400 AD significantly higher portions of ice rafted debris and high planktic foraminifer fluxes suggest that the site was located in the region of a seasonal highly fluctuating sea ice margin. A sharp reduction in planktic foraminifer fluxes around 800 AD and after 1730 AD indicates cool summer conditions with major influence of sea ice/icebergs. High amounts of the subpolar planktic foraminifer species *Turborotalia quinqueloba* in size fraction 150-250 µm indicate strengthened Atlantic Water inflow to the eastern Fram Strait already after ~1860 AD. Nevertheless surface conditions stayed cold well into the 20th century indicated by low planktic foraminiferal fluxes. Most likely at the beginning of the 20th century, cold conditions of the terminating Little Ice Age period persisted at the surface whereas warm and saline Atlantic Water already strengthened, hereby subsiding below the cold upper mixed layer. Surface sediments with high abundances of subpolar planktic foraminifers indicate a strong inflow of Atlantic Water providing seasonal ice-free conditions in the eastern Fram Strait during the last few decades.

Keywords

Late Holocene, Fram Strait, Atlantic Water, multiproxy, stable oxygen and carbon isotopes, planktic foraminifers

1. Introduction

In the recent climate discussion the Arctic Ocean has been identified as one of the most sensitive areas with respect to ongoing global warming processes. In particular, the term “Arctic amplification” has become popular when explaining the enforced warming in the Arctic. In high latitudes, greenhouse gas-induced rises in atmospheric temperatures generate a

lowering of the albedo due to sea ice loss. As a consequence, compared to the Northern Hemisphere as a whole, more heat is transported from the Arctic Ocean to the atmosphere, especially during winter (e.g., Manabe and Stouffer, 1980; Serreze et al., 2009). The Fram Strait is the only deepwater passage for relatively warm and saline Atlantic Water (AW) masses to enter the Arctic Ocean. While its western part is perennially ice-covered, Atlantic Water enters the Arctic Ocean through the eastern part of Fram Strait, keeping it ice-free all year (Fig. 1). Today, Fram Strait plays a crucial role for the heat budget and the sea ice extent of the Arctic. During the past few decades it has shown major variabilities in the flow strength of Atlantic Water (e.g., Karcher et al., 2003; Schauer et al., 2004). As a consequence, enhanced heat influx by Atlantic Water led to almost completely absence of ice in Kongsfjorden (Svalbard) during winter/spring 2006 (Hop et al., 2006) and subsequently to a delayed and reduced spring bloom (Hegseth and Tverberg, 2008). During the following two winters a reduced ice cover persisted which may be an indication for a warming of the entire fjord system that may have passed a tipping point (Hop et al., 2010) with most likely major impacts on the biological system.

Proxy data provide knowledge of past climate variability that is essential for understanding and modelling of current and future climate trends (Jones et al., 2001). In extending the record of climate variability beyond the era of instrumental measurements, proxy records provide information about the mechanisms, forcing factors, and spatial and temporal ranges of climatic variations (Houghton et al., 1996; Jones et al., 2001).

Terrestrial proxy studies and marine low-resolution proxy data reveal a pervasive cooling during the past two millennia in the Arctic realm that is mainly attributed to the orbitally driven reduction in summer insolation (Kaufman et al., 2009; Moberg et al., 2005). Beside the general cooling trend, climate fluctuations, in particular the Medieval Climate Anomaly (MCA) and the Little Ice Age (LIA), have been noticed in the North Atlantic region (e.g., Bjune et al., 2009; Eiríksson et al., 2006). Notably, it has been debated whether

temperatures during the MCA exceeded those of the warming in the past few decades and if there was a warming during the medieval at all (Broecker, 2001; Hughes and Diaz, 1994; IPCC, 2007; Moberg et al., 2005). In the Fram Strait area such climate variability is expressed in the glacier history on Svalbard. Studies on Svalbard glaciers have unveiled the Little Ice Age glaciation as the most extensive late-Holocene glacier advance recognized on Spitsbergen (Isaksson et al., 2005; Svendsen and Mangerud, 1997; Tarussov, 1992; Werner, 1993).

In this paper, we present high-resolution, multidecadal proxy records off West Spitsbergen where surface waters primarily are influenced by the relatively warm and saline Atlantic-derived water masses of the West Spitsbergen Current (WSC). While high-resolution marine proxy reconstructions are still lacking for the latest Holocene in the Arctic Ocean, a few studies are available from the Nordic Seas (e.g., Eiríksson et al., 2006; Klitgaard Kristensen et al., 2004; Sicre et al., 2008) and the Fram Strait (Bonnet et al., 2010). In reconstructing sea-surface temperatures (SST) by alkenones at the North Icelandic shelf, Sicre et al. (2008) found an abrupt increase of SST at ca 1000 AD, related to the onset of the MCA. A sharp cooling after ca 1350 AD is attributed to the beginning of the LIA (Sicre et al., 2008). Indicated by planktic foraminifer assemblages and planktic stable isotopes, Eiríksson et al. (2006) reported an overall cooling trend throughout the last ca 1000 years north of Iceland and at the Norwegian margin. Klitgaard Kristensen et al. (2004) indicate lower-than-present temperatures from 1225 to 1450 and 1650 to 1905 AD in the eastern Norwegian Sea, the latter interval attributed to the Little Ice Age. The past 80 years have been described as warmest within the last 800 years period at the Norwegian margin (Klitgaard Kristensen et al., 2004).

A marine record from the West Spitsbergen continental margin with similar time resolution was obtained from station JM06-WP-04 MC (78°54’N, 6°46’E) in the very vicinity to our study site (Bonnet et al., 2010). Interrupted by short cooling pulses, conditions warmer

than present were reconstructed for near-surface waters before ~1650 AD by studies on dinocyst assemblages (Bonnet et al., 2010). Warmest sea surface temperatures with ice-free conditions were detected in this study around ~1320 cal years BP (ca 630 AD). During the last ~300 cal years BP Bonnet et al. (2010) indicated a cooling trend of surface waters with significantly increasing sea ice coverage.

In the eastern Fram Strait Atlantic Water submerges beneath a less saline and cooler upper mixed water layer (e.g., Ślubowska et al., 2005) keeping a large part of eastern Fram Strait ice-free throughout the year. Dinocyst assemblages mainly reflect surface ocean conditions (e.g., Serjeant, 1974; Taylor, 1987). Reconstructing the past behaviour of the complex ocean current system in the eastern Fram Strait is essential to understand ongoing changes in the Arctic Ocean. It requires reliable indicators of both, surface and subsurface water layers. Planktic foraminifers are a useful tool to detect conditions in different water depths. While the polar species *Neogloboquadrina pachyderma* calcifies its tests at the base of the surface water layer in 50 to 200 m water depth the subpolar species *Turborotalia quinqueloba* is known as a symbiont-bearing surface dweller (Simstich et al., 2003) bound to seasonally open conditions (Kucera et al., 2005). By using the isotopic composition of planktic and benthic foraminifers, planktic foraminiferal assemblages and lithogenic parameters, our study tracks variations in the intensity of Atlantic Water inflow and changes in the sea ice extent in the eastern Fram Strait, and hence, variations of the heat transfer to the Arctic Ocean during the last two millennia.

2. Regional setting

In the eastern Fram Strait, relatively warm and saline water masses deriving from the North Atlantic Current are carried poleward with the WSC into the Arctic basin (Quadfasel et al., 1987; Fig. 1). Part of the inflowing Atlantic Water continues north and west of the Yermak Plateau as the Yermak Branch, whereas the Svalbard Branch transports these water

masses eastwards into the Arctic Ocean (Manley, 1995; Rudels et al., 2000; Saloranta and Haugan, 2001). The East Spitsbergen Current (ESC) carries cold water and sea ice from the Arctic Ocean southward along the east coast of Svalbard to the south and west around Spitsbergen (Hopkins, 1991; Loeng, 1991). Part of it, eventually mixing with brine-enriched shelf water from Storfjorden (Quadfasel et al., 1988; Schauer, 1995), joins the WSC to the west (Hopkins, 1991, and references therein), thereby cooling and freshening the north-flowing Atlantic Water masses. The western part of the Fram Strait is controlled by the southward directed East Greenland Current (EGC), which transports cold fresh water and sea ice along the Greenland continental slope into the Nordic Seas where minor currents such as the Jan Mayen Current and the East Icelandic Current branch off eastward (Fig. 1; Hopkins, 1991).

The hydrography of the Fram Strait controls the persistence of a specific seasonal sea ice distribution pattern (Fig. 1). The western part in the vicinity of the Greenland coast is perennially covered by sea ice, whereas the eastern Fram Strait has seasonally varying ice conditions. Large areas in the west and north of Svalbard stay ice-free all year, affected by the warmer, higher saline Atlantic Water inflow (Aagaard et al., 1987; Rudels et al., 2000).

Norwegian Sea Deep Water (NSDW), that originates from thermohaline processes in the Greenland Sea, flows northwards underneath the WSC in the eastern Fram Strait (Swift and Koltermann, 1988; Schlichtholz and Houssais, 1999).

During the past ~150 years, the investigated site experienced alternating positions of the winter sea ice margin (Vinje, 2001). Thus, similar sea ice variability can be anticipated also for the last two millennia. Today, the study site is situated under seasonal ice-free conditions, impacted by the Atlantic Water-bearing WSC (Fig. 1).

3. Materials and methods

The 46 cm long sediment core (box core) MSM5/5-712-1 was retrieved from the western Svalbard continental margin (78°54.94' N, 6°46.04' E, 1490.5 m water depth, Fig. 1) during cruise leg MSM5/5 with RV „Maria S. Merian" in summer 2007.

Sampling was carried out every 0.5 cm throughout the core section for the analysis of planktic and benthic isotopes, for ice rafted debris (IRD) and grain size studies, and for the investigation of planktic foraminiferal assemblages in the 100-250 µm size fraction. Studies on planktic foraminifer assemblages in size fraction 150-250 µm and the reconstruction of sea surface temperatures and salinities were carried out in 0.5 cm steps in the upper 5 cm and every 1 cm in the remainder of the record. Planktic foraminifer species involve *Neogloboquadrina pachyderma*, *Turborotalia quinqueloba*, *Neogloboquadrina incompta*, *Globigerinita* sp., and *Globigerina bulloides*. We refer to the term *N. incompta* following Darling et al. (2006) who identified *N. pachyderma* (sinistral coiling) (now redefined to *N. pachyderma*) and *N. pachyderma* (dextral coiling) (redefined to *N. incompta*) as different species. The samples were freeze-dried and wet-sieved in deionised water through a 63 µm-sized mesh to remove clay and silt material. Dry bulk density was determined every 5 cm from defined 10 cm^3 samples.

Age control is based on five accelerator mass spectrometry (AMS) radiocarbon dates published in Spielhagen et al. (2011) (Table 1). Analyses were conducted at the Leibniz Laboratory of Kiel University using ca 10 mg of $CaCO_3$. Except for the surface sample all measurements were carried out on a single species *N. pachyderma*. Due to an insufficient amount of *N. pachyderma* additional planktic foraminifer species including *T. quinqueloba*, *G. bulloides*, and *N. incompta* were used for age determination of the surface sample. Furthermore the amount of Rosa Bengal stained benthic foraminifers was counted in the surface sample to estimate the quantity of living species immediately after core recovery and thus to confirm a possible modern age of the surface sample.

The radiocarbon dates were converted to calendar years BP (Present = AD 1950) applying the calibration software Calib version 6.0 (Stuiver and Reimer, 1993) with the use of the Marine09 calibration data set (Reimer et al., 2009), including a reservoir correction of ~400 years. Chronology is established using the calibrated calendar ages and assuming uniform sedimentation rates between them by linear interpolation. If not marked specifically all ages discussed here are given in calendar years AD. Since the age-depth model reveals bidecadal time-resolution we rounded all ages accordingly. We refrained from applying a regional average correction ΔR value since all values provided by the Marine Reservoir Correction Database in CALIB (http://calib.qub.ac.uk/marine/) were obtained from the shallow Svalbard coast area and therefore seem not appropriate as a suitable ΔR value for our site at ca 1500 m water depth. Nevertheless we are aware of a possible shift to younger ages due to the ΔR effect when applying our age-depth model.

For investigation of ice rafted debris (IRD) lithic fragments were counted on a representative split (> 100 grains) of the 150-250 µm size fraction. No significant changes in lithology were noted throughout the core and thus we present undifferentiated IRD data only. IRD fluxes were calculated based on dry bulk density values and linear sedimentation rates. Sortable silt mean grain size analysis was carried out every 1 cm using an aliquot of the freeze-dried samples. To remove carbonate and organic matter samples were treated with acetic acid and hydrogen peroxide, respectively. After adding sodium polyphosphate for better dispersion the freeze-dried samples were put on a shaker for at least 24 hours. Measurements were performed with a CILAS 1180 laser-diffraction particle analyser. The sortable silt mean grain size 10-63 µm (Robinson and McCave, 1994) was calculated using the entire granulometric data sets based on vol.%. When considering a certain contamination of the current-transported sortable silt with sea ice-transported silt, it is likely that a fine sortable silt content results from less coarser silt material due to less sea ice melting (Hass, 2002).

The planktic foraminifer *N. pachyderma* and the benthic foraminifer *Cibicidoides wuellerstorfi* were chosen for stable oxygen and carbon isotope analyses because of their continuous presence in the sediment core. In order to prevent possible ecological biases of different morphotypes (Healy-Williams, 1992) only "square-shaped" (four-chambered) specimens of *N. pachyderma* were used. Analysis was performed at the IFM-GEOMAR Stable Isotope Lab using a Finnigan MAT 253 mass spectrometer system and a Kiel IV Carbonate Preparation Device. The carbonate was treated with orthophosphoric acid at 70°C. The analytical accuracy is 0.06‰ for $\delta^{18}O$ and 0.03‰ for $\delta^{13}C$ or smaller. All measurements were calibrated to Pee Dee Belemnite (PDB) standard (international standard NBS 19). Oxygen isotope data of *C. wuellerstorfi* were corrected for their disequilibrium effect by +0.64‰ (Duplessy et al., 2002; Shackleton and Opdyke, 1973).

Planktic foraminiferal assemblages were studied on the size fractions 100–250 µm and 150-250 µm (see Spielhagen et al., 2011). A representative split of at least 300 planktic foraminiferal tests was counted and identified to species level. The fraction >250 µm was neglected due to an almost complete absence of planktic foraminifers. Planktic foraminifer fluxes were calculated on dry bulk density values and linear sedimentation rates (Spielhagen et al., 2011).

For calculation of sea surface temperatures (SST) we used the planktic foraminifer census data of size fraction 150-250 µm following the SIMMAX procedure of Pflaumann et al. (1996) (for details see Spielhagen et al., 2011). In order to reconstruct salinity variations we used the paleotemperature equation (O'Neil et al., 1969)

$$T = 16.9-4.38(\delta_c-\delta_w)+0.1(\delta_c-\delta_w)^2$$

to derive $\delta^{18}O$ of the ocean water (δ_w in V-SMOW) from SST used from our SIMMAX reconstruction (T) and our measured $\delta^{18}O$ values of *N. pachyderma* (δ_c). In order to derive

salinities from δ_w we applied a modern salinity/$\delta^{18}O$ correlation of the water column on the Western Svalbard margin from 100 to 500 m water depth, which covers the depth of the AW core within the WSC. Data from Frank (1996) and Meredith et al. (2001) were retrieved from the Global Seawater Oxygen-18 Database (Schmidt et al., 1999; Fig. 2):

$$\delta^{18}O = 0.471 * S - 16.195.$$

Overall, the applied data show a relative small range of variations. The observed correlation is very similar to a mixing line between Atlantic Water ($\delta^{18}O$ of 0.3‰ vs. SMOW; salinity 35.1) and measurements made for fjord waters at the Svalbard coast (100-500 m water depth in the nearby Kongsfjorden; MacLachlan et al., 2007). Here, freshwater mainly consists of glacial melt water and the mixing line with Atlantic Water reveals a relationship of $\delta^{18}O = 0.43 * S - 14.69$ (MacLachlan et al., 2007). Due to the similarity between mixing lines of water in the WSC and fjord waters (Fig. 2), we expect the glacier melt influence to cause variations seen in the modern inflow of AW in the eastern Fram Strait and suppose that glacial melt water also had some influence on the water masses at our investigated site.

The calculated salinity value of about 35.5 for the core top sample is slightly higher than a salinity of 35.1 seen in present-day Atlantic Water at this position (Fig. 4g). We correct our salinity calculations by a shift of -0.2‰ in foraminiferal $\delta^{18}O$ in order to fit present-day Atlantic Water salinity of 35.1. A $\delta^{18}O$ vital effect for *N. pachyderma* cannot explain the calculated high salinity values as estimates vary between 0.8 and 1.3‰ for the Arctic (Bauch et al., 1997; Kohfeld et al., 1996; Volkmann and Mensch, 2001) and 0.4‰ for the eastern Fram Strait (Spielhagen and Erlenkeuser; 1994). Instead a shift of -0.2‰ in foraminiferal $\delta^{18}O$ may be generated by a temperature shift of roughly 1°C in reconstructed relative to actual temperatures. A temperature shift at the core position may easily occur as temperatures

within the West Spitsbergen Current are rapidly decreasing northward (Saloranta and Haugan, 2004) and SIMMAX SST may still partly represent higher temperatures found upstream. Corrected foraminiferal $\delta^{18}O$ (-0.2‰ shift) are used for salinity reconstructions only, and for the interpretation of reconstructed salinities only salinity trends are used. We like to note that the calculated SSS values are not an independent proxy but rather a translation of measured planktic $\delta^{18}O$ values and calculated SIMMAX SST.

Based on the paleotemperature equation (O'Neil et al., 1969) present-day oxygen equilibrium calcite values were calculated for subsurface (50 to 200 m) and bottom (1000 to 1600 m) water depths, respectively (Frank, 1996; Meredith et al., 2001; Schmidt et al., 1999). Oxygen isotope values of seawater (in V-SMOW) were transferred into $\delta^{18}O$ (PDB) (Bemis et al., 1998).

4. Results and interpretation

4.1 Sedimentation rates and lithological variations

The stratigraphic record of box core MSM5/5-712-1 extends ca 2,000 years (Table 1, Fig. 3a, for details see Spielhagen et al., 2011). Linear sedimentation rates vary between 18 and 20 cm/kyr in the lower core section and are 28.3 cm/kyr after 1500 AD (Fig. 3b). The time span of each 0.5 cm thick sample slice ranges between 25.1 and 27.7 years until 1500 AD, and is 17.7 years/0.5 cm sample for the past ca 500 years. Time resolution of planktic foraminiferal investigation of size fraction 150-250 µm, of the SST and SSS calculations, and of the sortable silt varies between 50.3 and 55.4 years/1 cm sample in the lower core section. During the past 500 years sortable silt samples cover a time span of 35.3 years/1 cm sample whereas samples of planktic foraminiferal study of size fraction 150-250 µm and the SST and SSS calculations range between 35.3 (1500-1850 AD) and 17.7 (since 1850 AD) years/0.5 cm sample. Dry bulk density values and linear sedimentation rates were used to calculate accumulation rates, which vary between 11.1 and 17.7 g/cm^2*kyr.

On a sediment core from the same site (JM06-WP-04-MC, 78°54'N, 6°46' E) mean sedimentation rates of ~18 cm/kyr contrast high sedimentation rates for the uppermost 11.5 cm (between 30 an 50 cm/kyr) based on AMS-^{14}C and ^{137}Cs measurements (Bonnet et al., 2010; Carignan et al., 2008). The high uppermost sedimentation rates have been attributed to an increased proportion of the coarse material that might possibly result from increased ice rafting (Bonnet et al., 2010). The same applies to our record where high sedimentation rates in the uppermost ~15 cm correspond to higher input of IRD and coarse-grained material as well as higher planktic foraminifer fluxes (Fig. 4a, c). Carignan et al. (2008) measured the anthropogenic lead distribution of the upper 20 cm of the JM06-WP-04-MC sediment core. A systematic decrease of high ^{210}Pb and anthropogenically-induced, less radiogenic input within the uppermost sediment layers and constant concentrations below confirmed mixing effects caused by bioturbation in the uppermost 8 cm of the sediment core (Carignan et al., 2008). Thus, the obtained ^{210}Pb data could not be used to document sedimentation rates (Bonnet et al., 2010).

IRD flux is relatively low until ~1300 AD with average values of ca 1,500 grains/cm^2*kyr (Fig. 4c). After 1350 AD it increases significantly. Lowest fluxes occur between 100 and 400 AD while a maximum of more than 5,400 grains/cm^2*kyr is observed ~1890 AD.

The sortable silt mean grain size is comparably small (around 25 µm) during almost the whole core section (Fig. 4d). After 1920 AD it increases significantly with a maximum of 33 µm around 1950 AD. The modern value falls back to 28 µm (Fig. 4d). Since various influences on the sortable silt grain size e.g., by bottom currents, their sediment loads and by possible IRD contamination are not fully understood at the moment, we refrain from a detailed interpretation but draw our conclusions on the main trends seen in the sortable silt record.

The sand content (63-1000 µm) varies between 1.7 and 9.0% (Fig. 4e). Lowest portions not exceeding 2% coincide with those observed in the IRD flux at 100-400 AD. Since 1700 AD the sand content parallels the trend in IRD flux and increases with average values of more than 4.5%. It reveals its maximum of more than 9% in the surface sample.

4.2. Stable oxygen and carbon isotopes

Variations of planktic $\delta^{18}O$ values range between 3.0 and 4.0‰ (Fig. 4h). Episodes of outstanding heavy values of more than 3.6‰ occur at ~30, 750-820, 1570-1610, and 1930-1960 AD. Light intervals are observed at ~100-200 and 1730-1840 AD. Benthic $\delta^{18}O$ values range from 4.4 to 5.2‰ (Fig. 4j). Light values (<4.6‰) appear around 250 AD, before 1100 AD, and between 1850 and 1910 AD. The interval between 1930 and 1960 AD is characterized by a sharp increase to maximum values of up to >5.0‰. Thereafter, benthic $\delta^{18}O$ values shift to light values of up to 4.4‰.

Modern $\delta^{18}O$ equilibrium values of the 50 to 200 m water depth range between 2.93 and 4.16‰ covering not only the planktic $\delta^{18}O$ value measured on the surface sample but the entire planktic $\delta^{18}O$ range of the past 2000 years (Fig. 4h). The range of modern $\delta^{18}O$ equilibrium values from 1000 to 1600 m water depth is relatively narrow (4.41 to 4.61‰) and cannot explain a large part of the recorded benthic $\delta^{18}O$ values (Fig. 4j). However, the values of the uppermost samples are in good accordance to the present-day oxygen equilibrium range.

Planktic $\delta^{13}C$ values vary from 0.2 to 0.6‰ (Fig. 4i). Lightest values (<0.3‰) occur in the upper 4.5 cm, in agreement with Spielhagen and Erlenkeuser (1994) who reported modern planktic $\delta^{13}C$ of <0.4‰ in the eastern Fram Strait. Heavier values are noticed around 200 and between 1500 and 1800 AD. The benthic $\delta^{13}C$ record ranges between 0.7 and 1.3‰ (Fig. 4k).

Values are higher at ~750-920 and ~1600-1850 AD. Considerably lighter values occur in the uppermost core section comprising the past ca 100 years.

4.3. Planktic foraminifer diversity and flux

Planktic foraminiferal data and corresponding SIMMAX temperature reconstructions from core MSM5/5-712-1 were reported by Spielhagen et al. (2011) and are presented here to support conclusions from other proxies. On the western Svalbard margin the planktic foraminifer fluxes and percentages in the 100-250 µm size fraction are highly variable during the last 2,000 years (Fig. 4a, b). At ~1-700 and ~1350–1750 AD planktic foraminifer fluxes were high (mean values around 9,000 ind./cm^2*kyr) and fluctuated strongly (Fig. 4a). Lower and less fluctuating fluxes appeared at ~700-1350 AD (5,300 ind./cm^2*kyr on average) and ~1730-1950 AD (1,700 ind./cm^2*kyr on average).

Except for the core top section, percentages of *N. pachyderma* vary between 55 and 86% throughout the past two millennia (Fig. 4b). In the uppermost core section, subpolar planktic foraminifers up to 66% (Fig. 5b, c, 6c) characterize high planktic foraminifer fluxes (up to 15,500 ind./cm^2*kyr, Fig. 4a, 6b). Subpolar species include *T. quinqueloba*, *N. incompta*, *Globigerinita* sp., and *G. bulloides*. The main species are shown in Fig. 5b, c. *Globigerinita* sp. combines findings of *Globigerinita uvula* and *Globigerinita glutinata* which cannot always be differentiated when smaller than 150 µm. Subpolar planktic foraminifers are present throughout the whole core section (Fig. 6c). After ~1950 AD a drastic increase of *T. quinqueloba* up to 38% is observed in size fraction 100-250 µm, paralleled by increasing portions of *Globigerinita* sp., which reach up to values of 27% (Fig.5c; Spielhagen et al., 2011).

Previous investigations have demonstrated the advantage of employing small-sized fractions for paleoceanographic reconstructions (Kandiano and Bauch, 2002). Often, small specimens and juvenile forms of the planktic foraminifers *G. glutinata, G. uvula*, and *T.*

quinqueloba are not included in the analysis when using a coarser size fraction (e.g., Bauch, 1994; Carstens et al., 1997; Kandiano and Bauch, 2002). In size fraction 150-250 µm, average portions of 80% and 15% are noticed for *N. pachyderma* and *T. quinqueloba*, respectively (Fig. 5a, b). A significant increase in percentages of *T. quinqueloba* is reflected in both size fraction during the last few decades. The increased content of *T. quinqueloba* in size fraction 150-250 µm ~1930 AD is not seen in the 100-250 µm fraction due to higher percentages of small-sized *N. pachyderma* specimens.

4.4. Sea surface temperature and salinity reconstruction

SIMMAX results based on the planktic foraminifer assemblages in the 150-250 µm size fraction reveal higher summer SST between 650 and 1400 AD with maximum temperatures of 4.4°C (Fig. 4f). Highest SST are noticed from ~1800 AD to present time, with maximum temperatures (6°C) reconstructed from the sediment surface sample. They correspond well to instrumental measurements of summer temperatures in the planktic foraminifer habitat depth (50-200 m) of the Atlantic Water core (4 to 6°C) in the eastern Fram Strait (Fig. 4f; Spielhagen et al., 2011).

A peak in sea surface salinity of 35.0 similar to the modern one is recorded after 800 AD (Fig. 4g). Higher-than-modern-salinities are reconstructed after 1910 AD with a maximum salinity of 35.7 after ~1960 AD. Since salinities of more than 35.2 are not realistic for this area today, we refrain from a detailed interpretation of the reconstructed sea surface salinities. However, trends in the surface salinity record will be used for further interpretation.

5. Discussion

5.1. Neoglaciation trend and Atlantic Water inflow

Covering the last ca 2,000 years, our proxy data set suggests variable oceanographic and climatic conditions in the eastern Fram Strait, which we attribute to the variable strength

of Atlantic Water inflow and the position of the sea ice margin. Stepwise increasing IRD contents (Fig. 4c, 6a) unveil a background trend of increasing iceberg/sea ice abundance on the western Svalbard margin during the last two millennia. In high latitude areas, such an increase may reflect either warmer or cooler conditions. Glaciers can grow and discharge more icebergs both in warmer climates with more precipitation on the mountains (Nesje, 2009) and in cooler climates for which less snow melt in summer can be assumed. Coarse lithic particles may also be picked up by seasonal sea ice in littoral zones and released at the sea ice margin upon melting. During the late Holocene, decreasing solar insolation (e.g., Berger and Loutre, 1991) and increasing snow precipitation during generally milder winters in the high northern latitudes (Moros et al., 2004; Nesje et al., 2008) are attributed to a neoglaciation trend. It is pronounced in many terrestrial archives in northern Europe and Greenland (e.g., Bjune et al., 2009; Dahl and Nesje, 1996; Matthews et al., 2000; Nesje et al., 1991, 2000) and seems to have also affected marine sediments from the North Atlantic (e.g., Andrews, et al., 2009, 2010; Koç and Jansen, 2002; Jennings et al., 2002; Moros et al., 2004; Seidenkrantz et al., 2008). A stepwise IRD increase in our record confirms the neoglaciation trend (Fig. 6a) which, however, does not necessarily reflect a continuous cooling during the past two millennia. Although coldest conditions of our reconstruction are linked to the Little Ice Age period, we also observe cold conditions at the site between 700 and 900 AD indicated by low and less fluctuating planktic foraminifer fluxes and a dominance of polar planktic species (>70%, Fig. 6b, c).

Continuous abundance of the subpolar planktic foraminifer species *T. quinqueloba* indicates that Atlantic Water has been permanently present during the past two millennia at the West Spitsbergen continental margin. *T. quinqueloba*, today dominating the Atlantic-derived water masses of the WSC with >80% (Volkmann, 2000), never falls below 8% in the 100-250 µm size fraction (Fig. 5b). Further south, Andersson et al. (2003) reported the uninterrupted abundance of *T. quinqueloba* for the past 3,000 years from the Vøring Plateau.

Ślubowska-Woldengen et al. (2007) found evidence for a continuous presence of Atlantic Water at the sea floor on the western and northern Svalbard margins since approximately 15,000 cal year BP.

5.2. Paleoceanographic reconstruction and climatic implications

On a transect across the Fram Strait, Hebbeln and Wefer (1991) found highest particle flux rates at the sea ice margin, characterized by maximum and strongly fluctuating planktic foraminifer fluxes (Carstens et al., 1997). Accordingly, we use variations in the planktic foraminifer flux record to subdivide our record into seven time intervals (Fig. 4). High and strongly variable fluxes at 1 - 700 AD and 1350 - 1730 AD are interpreted as indicative of a fluctuating ice margin located close to the study site (for detailed discussion see Zamelczyk et al., in prep.). A proximity to the ice margin is also inferred from increased IRD fluxes at 400-700 AD and after 1350 AD which indicate periods of prolonged sea ice melt. Lower and less variable planktic foraminifers flux rates characterize three intervals, the first two also displaying low IRD fluxes. For these periods ~120 BC to 1 AD, 700 to 1350 AD, and ~1730 to 1900 AD we propose more stable conditions. The interval after ~1900 AD has several special characteristics and is treated separately.

5.2.1.Time interval ~120 BC and ~1 AD

From ~120 BC to 1 AD the studied sediments are characterized by low subpolar planktic foraminifer percentages and low planktic foraminifer fluxes, medium high IRD fluxes, and slightly increasing planktic and benthic $\delta^{18}O$ and $\delta^{13}C$ values (Fig. 4, 6). The microfossil and IRD proxies point to rather cool conditions with possibly extended seasonal ice coverage. Increasing planktic $\delta^{18}O$ and $\delta^{13}C$ values may result from a progressively cooling and moderately well-ventilated environment in the upper water column, consistent with a south-easterly extension of Polar Water in the Fram Strait. Intermediate water

conditions at the Western Svalbard margin may have been influenced by enhanced sea ice formation from cool, salty surface waters in the Barents Sea, leading to an admixture of high-density brines with high $\delta^{18}O$ and $\delta^{13}C$ values to the intermediate and deeper waters, as proposed by Rasmussen and Thomsen (2009) for earlier parts of the Holocene.

5.2.2. Time interval ~1 AD to ~700 AD

Between 1 and 700 AD, strong fluctuations in the percentages and total fluxes of planktic foraminifers indicate a varying intensity of AW inflow (Fig. 6b, c). Highest particle fluxes with significant fluctuations at the sea ice margin in the Fram Strait are evidence of a summer sea ice margin prevailing over the investigated site. This is indicated particularly after 400 AD by high IRD contents (Fig. 4c, 6a). *N. pachyderma* dominated the planktic foraminifer fauna, but a greater influence of the subpolar planktic foraminifer species (up to 42%) suggests temporarily a stronger impact of Atlantic Water to the site (Fig. 6c). Reconstructed summer SST are slightly increasing until ~700 AD with a peak of 4.1°C around 520 AD (Fig. 6g).

Between 100 and 300 AD low planktic and benthic $\delta^{18}O$ may indicate increased temperatures and a strengthened AW advection that may also have affected the bottom water layer. As was shown by Karcher et al. (2003) and Schauer et al. (2004) Atlantic Water warming during the past decades has been caused not only by increased heat transport but also by stronger flow and increased volume transport. Recent vertical variability of the AW layer has been demonstrated in south-eastern Fram Strait (Schlichtholz and Goszczko, 2006). For the past we consider a similar increase in AW volume to likely result in a downward expansion of AW possibly also affecting the bottom water layers at our site.

Intensified AW inflow is furthermore supported by increased portions of subpolar planktic foraminifers (up to 40%) and high planktic $\delta^{13}C$ values around 200 AD which may suggest *N. pachyderma* migrating to cooler surface waters with a more suitable, better-

ventilated near-surface habitat (Carstens and Wefer, 1992, Volkmann, 2000). Raised planktic foraminifer fluxes (>12,500 individuals/cm^2*kyr) indicate that the ice margin probably had prevailed close to the site. In the eastern Fram Strait, Bonnet et al. (2010) reported surface water conditions between 500 and 650 AD as warm as during the modern interval (Fig. 6g). Although we find a peak in subsurface water temperatures around 520 AD, portions of *N. pachyderma* at ~550 and ~650 AD vary between 60 to 80%, (Fig. 4b, 5a, b) indicating strong climate fluctuations most likely associated with a position close to the summer sea ice margin (Hebbeln and Wefer, 1991; Carstens et al., 1997).

5.2.3. Time interval ~700 to ~900 AD

Between 700 and 900 AD percentages of *N. pachyderma* (72-80%) in both size fractions (Fig. 5a) and low planktic foraminifer fluxes (<5,000 ind./cm^2*kyr) (Fig. 6b) indicate rather cool conditions. Consistently, Bonnet et al. (2010) reported a cooling pulse in surface waters ~750 AD indicated by dinocyst assemblages (Fig. 6g). Cold surface conditions are supported by high planktic $\delta^{18}O$ values. However, considering a certain salinity effect, high planktic $\delta^{18}O$ and decreasing planktic $\delta^{13}C$ are likely to mirror the subsurface Atlantic Water signature reported by Spielhagen and Erlenkeuser (1994) and may thus likely be attributed to increased AW advection and stronger stratification. Strengthened AW inflow is furthermore supported by a local maximum (20%) of *T. quinqueloba* (subpolar) content in size fraction 150-250 µm ~800 AD (Fig. 6d) and its associated higher SST and SSS (Fig. 6g, h). The 100-250 µm fraction is represented by a high *N. pachyderma* content of conspicuously low variability (75 ± 2%) and a subpolar foraminifer content of about 28% (Fig. 6c). It seems therefore likely that the subsurface advection of Atlantic Water carried allochthonous subpolar species to the site, while the dominance of *N. pachyderma* might be associated with growth of autochthonous *N. pachyderma* within locally cold surface conditions. Nørgaard-Pedersen et al. (2003) reported an overestimation of SIMMAX-derived

sea surface temperatures for the western Fram Strait where relatively warm, high-density surface water with 'warm' planktic foraminifers submerges below colder, low salinity and low-density surface water. A similar situation may have been present in the eastern Fram Strait between 700 and 900 AD. Such strong surface-to-subsurface water differences have both past and present analogues. From low biological productivity but significant presence of AW, indicated by benthic foraminifera, Ślubowska et al. (2005) concluded that strongest subsurface influx of Atlantic-derived water took place below a sea ice-covered surface at the northern Svalbard margin during the Bølling-Allerød interstadial. Bauch et al. (1997) described a similar situation for the modern northern Nansen Basin with a core of Atlantic Water overlain by a thick halocline and summer sea ice coverage of about 80-90%.

5.2.4. Time interval ~900 to ~1350 AD

Between ~900 and 1350 AD slightly lower and significantly less variable planktic foraminifer fluxes point to more stable conditions than during the preceding interval ~1 to 700 AD, coinciding with higher sea surface temperatures and salinities at around ~1000 AD and ~1300-1350 AD (Fig. 6b, g, h). Reconstructed warmer SST concur with increased percentages of subpolar species (37%) in both size fractions (Fig. 6d, g). Lower IRD fluxes suggest ice-free conditions during most of the year, possibly linked to a strengthened AW inflow. Planktic $\delta^{13}C$ values fluctuate between 0.3 and 0.57‰ and may be associated with a migration of *N. pachyderma* to variable water depths with optimal living conditions (Carstens and Wefer, 1992). Increased percentages of *T. quinqueloba* at ~1000 to 1200 AD and ~1300 to 1350 AD especially noted in the 150-250 µm size fraction (Fig. 6d) may point to strengthened inflow of Atlantic-derived water.

Warmer conditions since ~1000 AD are consistent with many studies from the North Atlantic that have documented the Medieval Climate Anomaly (MCA) (e.g., Lamb, 1965; Dahl-Jensen et al., 1998; Moberg et al., 2005). According to the IPCC and references therein

(2007) the medieval warmth was heterogeneous in terms of its precise timing and regional expressions. Although there is not enough evidence available, the authors of the IPCC (2007) acknowledge that the warmest period prior to the 20th century likely occurred between 950 and 1100 AD. This is consistent with our reconstruction of warm conditions lasting from ~1000 to 1200 AD.

Warmer conditions ceased after ~1200 AD when planktic foraminifer fluxes decreased and portions of *N. pachyderma* increased to >70%. An associated cooling pulse was also detected by Bonnet et al. (2010) at ~1150 AD in the surface water layer (Fig. 6g). Consistently, in our record decreasing SST and SSS after ~1150 AD (Fig. 6g, h) infer an influence of the mixed water layer which could be linked to decreasing planktic $\delta^{13}C$ values after 1250 AD pointing to a migration of *N. pachyderma* to greater water depth (Carstens et al., 1997). A drastic decrease in sea surface salinity between 1200 and 1400 AD is also supported by Bonnet et al. (2010) (Fig. 6h). After 1300 AD increased subpolar planktic foraminifers and planktic foraminifer fluxes suggest warmer conditions returning to the site but may also be attributed to more sea ice marking the transition to colder conditions of the subsequent Little Ice Age period.

Reconstructed warm conditions and strong AW impact in the North Atlantic domain during the MCA exhibit dating discrepancies which however could be induced by regionalism, uncertainties in age models, or different sensitivities of the applied proxies (Bonnet et al., 2010). On the Vøring Plateau, Andersson et al. (2003) indicated a warmer period around 1200-1400 AD while on the Norwegian margin Berstad et al. (2003) reported the MCA before 1400 AD. From benthic stable isotopes Eiríksson et al. (2006) determined the MCA at the Norwegian margin to the interval 900-1400 AD. North of Iceland Sicre et al. (2008) assigned a warming between 1000 and 1350 AD to stronger heat transport across Denmark Strait by the North Icelandic Irminger Current. In essence, the relatively warm

period in our Fram Strait record is thus in good correlation to other reconstruction from the Nordic Seas area.

5.2.5. Little Ice Age Period I (~1350 to ~1730 AD)

Representing the early phase of the LIA, the period between ~1350 and 1730 AD is characterized by highly variable planktic foraminifer fluxes and high variations of *N. pachyderma* abundance (Fig. 6b, c). Records from the North Atlantic reveal the LIA commencing mainly between 1300 and 1400 AD (Andersson et al., 2003; Berstad et al., 2003; Eiríksson et al., 2006). Svalbard ice cores displayed a significant cooling not before 1500 AD (Isaksson et al., 2005).

Increasing IRD contents indicate a major importance of sea ice/icebergs at the investigated site. Increasing planktic $\delta^{13}C$ values (up to 0.56‰) approach the high $\delta^{13}C$ signal known from Arctic waters (>0.4‰, Spielhagen & Erlenkeuser, 1994) and indicate that under a permanent ice cover *N. pachyderma* may have migrated to better-ventilated near-surface waters for reasons of food availability (Volkmann, 2000). Planktic foraminifer assemblages in both size fractions and the SST based on the size fraction 150-250 µm (3.3°C) suggest varying but prevalently cool conditions (Fig. 6c, d, g). The heavy planktic $\delta^{18}O$ signal at ~1600 AD (Fig. 6e) is likely associated with a strong cooling pulse. Bonnet et al. (2010) observed a freshwater peak in surface waters during that time (Fig. 6h). In contrast, summer sea surface salinities calculated on the basis of planktic $\delta^{18}O$ and SIMMAX-derived temperatures (see 3.) reveal high values and suggest strengthened AW inflow at ~1600 AD. Intensified AW inflow, however, would be linked to warmer temperatures. Instead, all other proxies reveal cool conditions. Thus, we render our calculated high SSS values erroneous for this time interval and question that the modern salinity/$\delta^{18}O$ relation on which our SSS estimation is based is applicable around 1600 AD. A cold upper mixed water layer and entrained sea ice may have produced the heavy $\delta^{18}O$ values of *N. pachyderma*. In contrast,

SIMMAX SST calculations are based on planktic foraminiferal assemblages which are to a certain part transported with the warm Atlantic subsurface water from the south, therefore likely suggesting warmer temperatures than those which actually occurred at the site.

We rely on the calculated SSS trends further on since for all other intervals discussed here the obtained salinity values correspond well to our proxy interpretation. The invalidity of the obtained modern salinity/$\delta^{18}O$ relationship around 1600 AD seems to be an exception which is furthermore supported by a coinciding peak in benthic $\delta^{13}C$ values. It remains speculative what caused the modification of inflowing water masses. It may have been induced by cold lateral advections, possibly originating from brine formation in the Storfjorden area (Rasmussen and Thomsen, 2009).

From dinocyst assemblages Bonnet et al. (2010) detected a major transition to colder conditions within the surface water layer and increased sea ice cover around 1650 AD (Fig. 6g). The apparent offset in the timing of this drastic cold spell between the record of Bonnet et al. (2010) and our data set is most probably a problem of the different core chronologies. Both proxies confirm a shift to colder conditions in the surface and subsurface water layer which point to a major cold event affecting a large part of the entire water column. We note that from a combination of northern hemispheric low-resolution proxies and treering-data Moberg et al. (2005) concluded on minimum temperatures for the Little Ice Age period around 1600 AD.

5.2.6. Little Ice Age Period II (after ~1730 AD)

Similar to our findings, Andersson et al. (2003) found a two-phase LIA with cooling events centred around 1600 and 1900 AD. A second phase of the Little Ice Age is inferred from gradually decreasing planktic foraminifer fluxes and high percentages of *N. pachyderma* (64 to 78%) after 1730 AD (Fig. 6b, c). IRD contents slightly decrease between ~1750 and 1820 AD (Fig. 6a) and point to sea ice coverage due to restricted dispersion of ice-transported

material into the water (Hebbeln and Wefer, 1991). Low sortable silt mean size values are potentially linked to a weakened intermediate and deepwater circulation in the Norwegian-Greenland-Sea where the silt-transporting deepwater is produced. Low sortable silt mean size values from ~1700 to 1900 AD (Fig. 4d) thus possibly indicate a weakened meridional overturning circulation (MOC) during the Little Ice Age caused by massive intrusion of freshwater and sea ice from the Arctic (after Sicre et al., 2008). Alternatively, assuming a certain contamination of current-transported sortable silt with sea ice-transported silt, it is likely that the low sortable silt mean size values recorded from ~1700 to 1900 AD (Fig. 4d) result from less coarser silt material due to less sea ice melting.

After ~1830 AD the IRD flux continuously increased. Concurrently, planktic foraminifer fluxes reveal lowest values between ~1850 and 1950 AD (750 to 2500 ind./cm^2*kyr). All these findings are best explained by cool conditions with extensive sea ice cover and an increased number of icebergs resulting from glacier growth on Svalbard. Indeed, historical observations from the archipelago corroborate a sea ice-dominated regime in the Fram Strait during the late LIA (e.g., Divine and Dick, 2006). For the period before 1920 AD sea ice reconstructions by Vinje (1999, 2001) showed intervals of heavy sea ice interrupted by periods of modest sea ice conditions. A possible impact of glacial melt water is supported by the comparison between mixing lines of modern water in the WSC (see 3.) and fjord waters at the Svalbard coast (MacLachlan et al., 2007), the latter mainly consisting of freshwater originating from glacial melt water (Fig. 2). Despite of the distance to the fjords, we suppose that glacial melt had some influence also on the water masses at our core site. Svalbard ice core studies revealed coldest conditions of the Little Ice Age for the period ~1760 to 1900 AD (Isaksson et al., 2005). Little Ice Age moraines on Svalbard have been widely described to represent the Holocene glacial maximum (Svendsen and Mangerud, 1997). Glacier advances during the Little Ice Age were reported for the Svalbard region (e.g., Humlum et al., 2005; Isaksson et al., 2005; Svendsen and Mangerud, 1997; Werner, 1993) and must have released

icebergs into Svalbard fjords. Thus, it seems likely that IRD transported with icebergs also reached the study site.

5.2.7. Modern warming

There are discrepancies in our records concerning the end of the LIA. The gradual increase of *T. quinqueloba* in size fraction 150-250 µm (38%) and the associated temperature and salinity reconstructions (Fig. 5b, 6d, g, h) suggest a strong intensity of Atlantic Water since ~1850 AD (see also Spielhagen et al., 2011). In contrast, planktic foraminifer fluxes of size fraction 100-250 µm increase only after ~1950 AD (Fig. 6b). Before 1930 AD light planktic $\delta^{18}O$ values are most likely attributed to a cold and fresh upper mixed water layer (Fig. 6e). A sudden change is observed around 1930 AD when both, planktic and benthic foraminifer tests display a short-lived but very strong increase in $\delta^{18}O$ (4.03 and 4.56‰, respectively, Fig. 6e), pointing to an event that obviously affected the entire water column. An abrupt warming around the 1930s followed a temperature minimum in 1917 AD initiating the early 20th century warming in the Arctic (Isaksson et al., 2005 and references therein, Polyakov et al., 2004; Fig. 6i). A significant warming in the 1930s is also known from instrumental data from Svalbard (e.g., Førland et al., 2009). In contrast, Klitgaard Kristensen et al. (2004) attributed $\delta^{18}O$ increases of ~0.3-0.6‰ around 1925 AD in two cores from the Norwegian Sea and adjacent fjords to a cold period at 1905-1925 AD in the Southern Norwegian Sea. Our $\delta^{18}O$ changes of >0.47‰ (planktic) and >0.5‰ (benthic) (Fig. 6e) may accordingly be interpreted as a cold spell. The maximum in $\delta^{18}O$, however, corresponds to high reconstructed SST and a peak in *T. quinqueloba* in size fraction 150-250 µm at ~1930 AD. We therefore rather suggest a significantly Atlantic Water pulse to have caused the high planktic and benthic $\delta^{18}O$ values, hereby affecting also bottom water layers. Simultaneously, a salinity effect on $\delta^{18}O$ is supported by high summer SSS pointing to strengthened AW

inflow. Low fluxes and relatively high percentages of *N. pachyderma* in size fraction 100-250 µm do, however, not support warmer conditions. We therefore assume high abundances of small-sized *N. pachyderma* most likely indicating locally limited foraminifer growth due to cold conditions at the surface. Most likely at the beginning of the 20th century, the surface layer may have been still impacted by a thick cold and fresh mixed water layer as a retarding effect of the terminating Little Ice Age while warm and saline Atlantic Water already strengthened, hereby subsiding below the cold upper mixed layer.

Variations in planktic foraminifer fluxes and percentages as well as two independent temperature reconstructions during the last 2,000 years have already been discussed with respect to the unprecedented warming after 1860 AD (Spielhagen et al., 2011). The drastic increase in subpolar planktic foraminifers is particularly attributed to significant increases in *T. quinqueloba* and *Globigerinita sp.* (Spielhagen et al., 2011; Fig. 5b, c). Svalbard ice core studies have elucidated the 20th century as the warmest century within at least the past 600 years (Isaksson et al., 2005). Changes occur in all studied proxies since 1950 AD (Fig. 6) and coincide with positive Atlantic Water temperature anomalies for the ca last 100 years in the Arctic Ocean (Polyakov et al., 2004; Fig. 6i) and a retreating sea ice margin in the Nordic Seas (Divine and Dick, 2006). High sea surface salinities and light planktic $\delta^{18}O$ values likely reflect warmer sea surface temperatures and strengthened AW inflow (Fig. 6e, h).

Stable high IRD fluxes indicate a high abundance of sea ice/icebergs after 1860 AD. A significant increase in sortable silt mean size (Fig. 4d) was likely caused by silt-sized IRD indicating a high impact of sea ice at the site. It may also point to a continuous strengthening of the MOC intensity (Sicre et al., 2008) linked to increased deepwater production in the Norwegian-Greenland Sea.

Planktic and benthic $\delta^{13}C$ values decreased during the last 100 years (Fig. 6f). Bauch et al. (2000) found *N. pachyderma* in the water column depleted in $\delta^{13}C$ compared to core top sediments in the Arctic Ocean. Considering the multidecadal resolution of our data set, low

$\delta^{13}C$ values could be reflected in planktic foraminifers of the uppermost sediment layer studied here, while they were not observed in surface sediments from the Arctic Ocean characterized by extremely low sedimentation rates. Olsen and Ninnemann (2010) discussed the global distribution of light $\delta^{13}C$ values in modern water masses which are strongly departing from preindustrial values due to the Suess effect which involves the anthropogenically induced addition of isotopically light fossil carbon to the carbon system. Our recorded low $\delta^{13}C$ values may therefore be attributed to the Suess effect.

It has been debated whether temperatures of the Medieval Climate Anomaly have been similar to those of the past 100 years (Broecker, 2001; Hughes and Diaz, 1994; IPCC, 2007). Regarding percentages of subpolar planktic foraminifers of the two periods (up to 37% during MCA, up to 66% during past 100 years; Fig. 5b, c) we conclude that temperatures of the MCA in the eastern Fram Strait were considerably lower than those of the 20th century. This is also shown by two independent temperature reconstructions of core MSM5/5-712-1 indicating that modern summer temperatures of the uppermost AW layer are >1.5°C higher than multidecadal mean temperature maxima during the MCA (Spielhagen et al., 2011).

5.3. Analogies and disparities to dinocyst-based reconstruction – apparent conflicts between surface and subsurface water indicators

Our proxy reconstruction based on planktic foraminifer assemblages, stable isotopes of planktic and benthic foraminifera, and lithic characteristics partly contradicts results of Bonnet et al. (2010) derived from dinocyst assemblages. Figure 6g and h show summer SST and SSS reconstructions obtained by Bonnet et al. (2010) along with those of the present study. SST by Bonnet et al. (2010) are significantly higher during the ~1650 AD so that differences to SST of this study can easily reveal up to 6°C. Also, fluctuations of SST revealed by Bonnet et al. (2010) are considerably higher. A major temperature drop initiating the Little Ice Age period after a relatively warm interval has been detected by Bonnet et al.

(2010) ~1650 AD, which we find in our record at least 300 years earlier. High fluctuations in SST (Bonnet et al., 2010) may indicate a fluctuating sea ice margin at the site, as it has been indicated by the present study ~1-700 AD and after ~1350 AD. There is agreement to data of Bonnet et al. (2010) about a cooling pulse around 750 AD, which may correspond to an observed cold spell in our record around 800 AD. As pointed out by Krawczyk et al. (2010), inconsistencies in proxy data comparison may arise from different living depths of the applied microfossil proxies. Due to their (direct or indirect) dependence on photosynthesis, most cyst-producing dinoflagellate species live in the upper mixed water layer (e.g., Serjeant, 1974; Taylor, 1987). In contrast, the main habitat of planktic foraminifers during summer is the subsurface layer of the WSC between 50 and 200 m water depth in the Fram Strait (Carstens et al., 1997; Volkmann, 2000). To explain diatom and dinoflagellate cyst records from outer Disko Bugt (West Greenland) inconsistent to North Atlantic climate variability (Moros et al., 2006; Seidenkrantz et al., 2008), Krawczyk et al. (2010) presented an alternative to the seesaw mechanism (e.g., Keigwin and Pickart, 1999). Increased melting of sea ice and the Greenland ice sheet during warmer intervals such as the MCA would result in an increased influx of cold and low-saline water at the surface, which would produce a diatom assemblage indicative of colder conditions (Krawczyk et al., 2010). In contrast, during cooler intervals, such as the LIA, reduced melting of sea ice would reduce dilution of the upper mixed layer and would thus lead to a relative increase of warmer species in the diatom assemblages (Krawczyk et al., 2010). Likewise, this mechanism could apply to dinoflagellates since they also reflect conditions in the uppermost water layers. In the eastern Fram Strait a ca 50-100 m thick surface water layer above the West Spitsbergen Current cools and freshens the underlying AW (Saloranta and Haugan, 2004). As Polyakov et al. (2004) have shown during increased AW inflow there is excess ice and freshwater transport through Fram Strait from the Arctic. Therefore we consider the reconstruction of Bonnet et al. (2010) to mainly to reflect the uppermost water variability possibly influenced by fluctuations of the fresh and cold

upper mixed layer. Our planktic foraminifer-based proxies mainly reflect subsurface conditions of the Atlantic Water masses submerging beneath the upper mixed layer. In particular, the early part of the Little Ice Age reveals clear contradictions between both reconstructions. For the interval between 1400 and 1650 AD Bonnet et al. (2010) find warm summer SST while we infer rather cool conditions with the sea ice margin prevailing over the site. Assuming a similar scenario as described by Krawczyk et al. (2010) relatively warm summer SST by Bonnet et al. (2010) would represent reduced melting of sea ice due to a colder period. In contrast, during the second part of the LIA, cold SST (Bonnet et al., 2010) agree with our reconstructed cold climate conditions. Persistently cold conditions may have caused a rather homogeneous thick cold surface water layer, which may be represented by both, planktic foraminifers and dinoflagellates during the later LIA. However, comparison between SSS and SST data from Bonnet et al. (2010) and from this study does not reveal a distinct relationship. Due to the complexity of water masses in the narrow Fram Strait we are thus not able to develop a clear anti-phase relationship of surface and subsurface indicating organisms similar to the one for West Greenland (Krawczyk et al., 2010) .

6. Conclusions

Our proxy data set suggests variable oceanographic and climatic conditions during the last ca 2,000 years in the eastern Fram Strait, which we attribute to the variable strength of Atlantic Water inflow and the position of the sea ice margin. Stepwise increasing IRD contents unveil a background trend of increasing iceberg/sea ice abundance confirming a neoglaciation trend known from other studies in the North Atlantic area. Atlantic Water has been permanently present as indicated by the continuous abundance of the subpolar planktic foraminifer species *T. quinqueloba* today indicative of Atlantic Water in the Fram Strait. A fluctuating ice margin was located close to the study site 1 - 700 AD and 1350 - 1730 AD inferred from high and strongly variable planktic foraminifer fluxes. A proximity to the ice margin is also inferred

from increased IRD fluxes at 400-700 AD and after 1350 AD which indicate periods of prolonged sea ice melt. During the Medieval Climate Anomaly lower and less variable planktic foraminifer fluxes point to more stable conditions which, however, varied between warmer (1000-1200 AD, after 1300 AD) and cooler (1200-1300 AD) periods. Two phases of the Little Ice Age period have been revealed. The first phase (ca 1350-1750 AD) had high planktic foraminifer fluxes pointing to cold conditions and a fluctuating sea ice margin at the site. After ca 1750 AD decreasing planktic foraminifer fluxes indicate very cold conditions. High IRD contents are attributed to heavy sea ice conditions found also in historical observations and instrumental records. IRD may have also been produced by melting Svalbard glaciers. Subpolar planktic foraminifers in the 150-250 µm fraction and planktic $\delta^{18}O$ values indicate strengthened Atlantic Water inflow after ca 1860 AD. However, low fluxes and planktic foraminifer assemblages of the 100-250 µm fraction suggest cool surface water conditions until the mid of the 20th century. Changes in all studied proxies indicate warmer temperatures for the past few decades (see Spielhagen et al., 2011) and coincide with positive Atlantic Water temperature anomalies and a retreating sea ice margin for the ca last 100 years (Divine and Dick, 2006; Polyakov et al., 2004, 2005).

Acknowledgements

The German Research Foundation (DFG) provided financial support of K. Werner and R. F. Spielhagen within the Priority Programme 1266 (INTERDYNAMIC, Project HOVAG). K. Zamelczyk was funded by the Norwegian Research Council through the research programs WARMPAST and SciencePub. For technical assistance on stable isotope measurements we are grateful to Lulzim Haxhiaj. We thank Henning A. Bauch and Nicolas Van Nieuwenhove for constructive comments and consultations on this manuscript. We wish to thank the science party and crew onboard RV “Maria S. Merian” during the expedition MSM5/5 for retrieving

the sediment core. Finally we appreciate the valueable suggestions and comments by two anonymous reviewers which greatly improved the manuscript.

References

Aagaard, K., Foldvik, A., Hillman, S., 1987. The West Spitsbergen Current: Disposition and Water Mass Transformation. Journal of Geophysical Research 92(C4), 3778-3784.

Andersson, C., Risebrobakken, B., Jansen, E., Dahl, S.O., 2003. Late Holocene surface ocean conditions of the Norwegian Sea (Vøring Plateau). Paleoceanography 18, 1044.

Andrews, J.T., Belt, S.T., Olafsdottir, S., Massé, G., Vare, L.L., 2009. Sea ice and marine climate variability for NW Iceland/Denmark Strait over the last 2000 cal. yr BP. The Holocene 19, 775-784.

Andrews, J.T., Jennings, A.E., Coleman, G.C., Eberl, D.D., 2010. Holocene variations in minderal and grain size composition along the East Greenland glaciated margin (ca 67°-70°N): Local versus long-distance sediment transport. Quaternary Science Reviews 29, 2619-2632.

Bauch, D., Carstens, J., Wefer, G., 1997. Oxygen isotope composition of living *Neogloboquadrina pachyderma* (sin.) in the Arctic Ocean. Earth and Planetary Science Letters 146, 47-58.

Bauch, D., Carstens, J., Wefer, G., Thiede, J., 2000. The imprint of anthropogenic CO_2 in the Arctic Ocean: evidence from planktic $\delta^{13}C$ data from watercolumn and sediment surfaces. Deep-Sea Research II 47, 1791-1808.

Bauch, H., 1994. Significance of variability in *Turborotalia quinqueloba* (Natland) test size and abundance for paleoceanographic interpretations in the Norwegian-Greenland Sea. Marine Geology 121, 129-141.

Bemis, B.E., Spero, H.J., Bijma, J., Lea, D.W., 1998. Reevaluation of oxygen isotopic composition of planktic foraminifera: Experimental results and revised paleotemperature equations. Paleoceanography 13, 150-160.

Berger, A., Loutre, M.F., 1991. Insolation Values for the Climate of the last 10 Million Years. Quaternary Science Reviews 10, 297-317.

Berstad, I.M., Sejrup, H.P., Klitgaard Kristensen, D., Haflidason, H., 2003. Variability in temperature and geometry of the Norwegian Current over the past 600 yr; stable isotope and grain size evidence from the Norwegian margin. Journal of Quaternary Science 18(7), 591-602.

Bjune, A.E., Seppä, H., Birks, B.J.B., 2009. Quantitative summer-temperature reconstructions for the last 2000 years based on pollen-stratigraphical data from northern Fennoscandia. Journal of Paleolimnology 41, 43-56.

Bonnet, S., de Vernal, A., Hillaire-Marcel, C., Radi, T., Husum, K., 2010. Variability of sea-surface temperature and sea-ice cover in the Fram Strait over the last two millennia. Marine Micropaleontology 74, 59-74.

Broecker, W.S., 2001. Was the Medieval Warm Period Global? Science 291, 1497-1499.

Carignan, J., Hillaire-Marcel, C., de Vernal, A., 2008. Arctic vs. North Atlantic water mass exchanges in Fram Strait from Pb isotopes in sediments. Canadian Journal of Earth Sciences 45, 1253-1263.

Carstens, J., Hebbeln, D., Wefer, G., 1997. Distribution of planktic foraminifera at the ice margin in the Arctic (Fram Strait). Marine Micropaleontology 29, 257-69.

Carstens, J., Wefer, G., 1992. Recent distribution of planktonic foraminifera in the Nansen Basin, Arctic Ocean. Deep-Sea Research 39, S507-S524.

Dahl, O.S., Nesje, A., 1996. A new approach to calculating Holocene winter precipitation by combining glacier equilibrium-line altitudes and pine-tree limits: a case study from Hardangerjokulen, central southern Norway. The Holocene 6, 381-398.

Dahl-Jensen, D., Mosegaard, K., Gundestrup, N., Clow, G.D., Johnsen, S.J., Hansen, A.W., Balling, N., 1998. Past Temperatures Directly from the Greenland Ice Sheet. Science 282, 268-271.

Darling, K.F., Kucera, M., Kroon, D., Wade, C.M., 2006. A resolution for the coiling direction paradox in *Neogloboquadrina pachyderma*. Paleoceanography 21, PA2011.

Divine, D.V., Dick, C., 2006. Historical variability of sea ice edge position in the Nordic Seas. Journal of Geophysical Research 111, C01001.

Duplessy, J.-C., Labeyrie, L., Waelbroeck, C., 2002. Constraints on the ocean oxygen isotopic enrichment between the Last Glacial Maximum and the Holocene: Paleoceanographic implications. Quaternary Science Reviews 21, 315-330.

Eiríksson, J., Bartels-Jónsdóttir, H.B., Cage, A.G., Gudmundsdóttir, E.R., Klitgaard Kristensen, D., Marret, F., Rodrigues, T., Abrantes, F., Austin, W.E.N., Jiang, H., Knudsen, K.-L., Sejrup, H.-P., 2006. Variability of the North Atlantic Current during the last 2000 years based on shelf bottom water and sea surface temperatures along an open ocean/shallow marine transect in western Europe. The Holocene 16(7), 1017-1029.

Førland, E.J., Benestad, R.E., Flatøy, F., Hanssen-Bauer, I., Haugen, J.E., Isaksen, K., Sorteberg, A., Ådlandsvik, B., 2009. Climate development in North Norway and the Svalbard region during 1900-2100. Rapportserie 128, Norsk Polarinstitutt Tromsø, Norway.

Frank, M., 1996. Spurenstoffuntersuchungen zur Zirkulation im Eurasischen Becken des Nordpolarmeeres. PhD thesis Ruprecht-Karls-Universität Heidelberg.

Hass, H.C., 2002. A method to reduce the influence of ice-rafted debris on a grain size record from northern Fram Strait, Arctic Ocean. Polar Research 21, 299-306.

Healy-Williams, N., 1992. Stable isotope differences among morphotypes of *Neogloboquadrina pachyderma* (Ehrenberg): implications for high-latitude palaeoceanographic studies. Terra Nova 4, 693-700.

Hebbeln, D., Wefer, G., 1991. Effects of ice coverage and ice-rafted material on sedimentation in the Fram Strait. Nature 350, 409-411.

Hegseth, E.N., Tverberg, V., 2008. Changed spring bloom timing in a Svalbard (high Arctic) fjord caused by Atlantic Water inflow? SCAR/IASC IPY Open Science Conference July 8-11, 2008, St Petersburg, Russia.

Hop, H., Falk-Petersen, S., Svendsen, H., Kwasniewski, S., Pavlov, V., Pavlova, O., Søreide, J.E., 2006. Physical and biological characteristics of the pelagic system across Fram Strait to Kongsfjorden. Progress in Oceanography 71, 182-231.

Hop, H., Cottier, F., Falk-Petersen, S., Tverberg, V., Kwasniewski, S., Welcker, J., Moe, B., Hegseth, E.N., Gerland, S., Walczowski, W., Dalpadado, P., Klitgaard Kristensen, D., Berge, J., Lydersen, C., Kovacs, K.M., Weslawski, J.M., Gabrielsen, G.W., 2010. Has Kongsfjorden in Svalbard passed a tipping point for persistent change in the marine ecosystem? Arctic Frontiers Conference, Jan 24-29, 2010, Tromsø, Norway.

Hopkins, T.S., 1991. The GIN Sea - A synthesis of its physical oceanography and literature review 1972-1985. Earth-Science Reviews 30, 175-318.

Houghton, J.T.(ed.), Meiro Filho, L.G., Callandar, B.A., Harris, N., Kattenburg, A., Maskell, K., 1996. Climate change 1995: the science of climate change. Cambridge University Press.

Hughes, M.K., Diaz, H.F., 1994. Was there a 'Medieval Warm Period', and if so, where and when? Climatic Change 26, 109-142.

Humlum, O., Elberling, B., Hormes, A., Fjordheim, K., Hansen, O.H., Heinemeier, J., 2005. Late-Holocene glacier growth in Svalbard, documented by subglacial relict vegetation and living soil microbes. The Holocene 15, 396-407.

IPCC, 2007. IPCC Fourth Assessment Report: Climate Change 2007. Contribution of Working Group I to the Fourth Assessment Report of the Intergovernmental Panel on Climate Change, 2007. Solomon, S., Qin, D., Manning, M., Chen, M., Marquis, M., Averyt, K.B., Tignor, M., Miller, H.L. (Eds.), Cambridge University Press. Cambridge, United Kingdom and New York, USA.

Isaksson, E., Kohler, J., Pohjola, V., Moore, J., Igarashi, M., Karlöf, L., Martma, T., Meijer, H., Motoyama, H., Vaikmäe, R., van de Wal, R.S.W., 2005. Two ice-core $\delta^{18}O$ records from Svalbard illustrating climate and sea ice variability over the last 400 years. The Holocene 15, 501-509.

Jakobsson, M., Macnab, R., Mayer, L., Anderson, R., Edwards, M., Hatzky, J., Schenke, H.W., Johnson, P., 2008. An improved bathymetric portrayal of the Arctic Ocean: Implications for ocean modelling and geological, geophysical and oceanographic analyses. Geophysical Research Letters 35, L07602.

Jennings, A.E., Knudsen, K.L., Hald, M., Vigen Hansen, C., Andrews, J.T., 2002. A mid-Holocene shift in Arctic sea-ice variability on the East Greenland Shelf. The Holocene 12, 49-58.

Jones, P.D., Osborn, T.J., Briffa, K.R., 2001. The Evolution of Climate Over the Last Millennium. Science 292, 662-667.

Kandiano, E.S., Bauch, H.A., 2002. Implications of planktic foraminiferal size fractions for the glacial-interglacial paleoceanography of the polar North Atlantic. Journal of Foraminiferal Research 32, 245-251.

Karcher, M.J., Gerdes, R., Kauker, F., Köberle, C., 2003. Arctic warming: Evolution and spreading of the 1990s warm event in the Nordic seas and the Arctic Ocean. Journal of Geophysical Research 108(C2), 3034.

Kaufman, D.S., Schneider, D.P., McKay, N.P., Ammann, C.M., Bradley, R.S., Briffa, K.R., Miller, G.H., Otto-Bliesner, B.L., Overpeck, J.T., Vinther, B.M., Arctic Lakes 2k

Project Members, 2009. Recent Warming Reverses Long-Term Arctic Cooling. Science 325, 1236-1239.

Keigwin, L.D., Pickart, R.S., 1999. Slope Water Current over the Laurentian Fan on Interannual to Millennial Time Scales. Science 286, 520-523.

Klitgaard Kristensen, D., Sejrup, H.P., Haflidason, H., Berstad, I.M., Mikalsen, G., 2004. Eight-hundred-year temperature variability from the Norwegian continental margin and the North Atlantic thermohaline circulation. Paleoceanography 19, 2007.

Koç, N., Jansen, E., 2002. Holocene Climate Evolution of the North Atlantic Ocean and the Nordic Seas - a Synthesis of New Results, in: Wefer, G., Berger, W., Behre, K.-E., Jansen, E. (Eds.), Climate Development and History of the North Atlantic Realm. Springer-Verlag, pp. 165-177.

Kohfeld, K.E., Fairbanks, R.G., Smith, S.L., Walsh, I.D., 1996. *Neogloboquadrina Pachyderma* (sinistral coiling) as Paleoceanographic Tracers in Polar Oceans: Evidence from Northeast Water Polynya Plankton Tows, Sediment Traps, and Surface Sediments. Paleoceanography 11, 679-699.

Krawczyk, D., Witkowski, A., Moros, M., Lloyd, J., Kuijpers, A., Kierzek, A., 2010. Late-Holocene diatom-inferred reconstruction of temperature variations of the West Greenland Current from Disko Bugt, central West Greenland. The Holocene 20(5), 659-666.

Kucera, M., Weinelt, M., Kiefer, T., Pflaumann, U., Hayes, A., Weinelt, M., Chen, M.-T., Mix, A.C., Barrows, T.T., Cortijo, E., Duprat, J., Juggins, S., Waelbroeck, C., 2005. Reconstruction of sea-surface temperatures from assemblages of planktonic foraminifera: multi-technique approach based on geographically constrained calibration data sets and its application to glacial Atlantic and Pacific Oceans. Quaternary Science Reviews 24, 951-998.

Lamb, H.H., 1965. The early Medieval Warm Epoch and its sequel. Palaeogeography, Palaeoclimatology, Palaeoecology 1, 13-37.

Loeng, H., 1991. Features of the physical oceanographic conditions of the Barents Sea, in: Sakshaug, E., Hopkins, C.C.E., Øritsland, N.A. (Eds.), Proceedings of the Pro Mare Symposium on Polar Marine Ecology, Trondheim, 12-16 May 1990. Polar Research 10, 5-18.

MacLachlan, S.E., Cottier, F.R., Austin, E.N.A., Howe, J.A., 2007. The salinity: $\delta^{18}O$ water relationship in Kongsfjorden, western Spitsbergen. Polar Research 26, 160-167.

Manabe, S., Stouffer, R.J., 1980. Sensitivity of a Global Climate Model to an Increase of CO_2 Concentration in the Atmosphere. Journal of Geophysical Research 85(C10), 5529-5554.

Manley, T.O., 1995. Branching of Atlantic Water within the Greenland-Spitsbergen Passage: An estimate of recirculation. Journal of Geophysical Research 100(C10), 20627-20634.

Matthews, J.A., Dahl, S.O., Nesje, A., Berrisford, M.S., Andersson, C., 2000. Holocene glacier variations in central Jotunheimen, southern Norway based on distal glaciolacustrine sediment cores. Quaternary Science Reviews 19, 1625-1647.

Meredith, M., Heywood, K., Dennis, P., Goldson, L., White, R., Fahrbach, E., Schauer, U., Østerhus, S., 2001. Freshwater fluxes through the Western Fram Strait. Geophysical Research Letters 28, 1615-1618.

Moberg, A., Sonechkin, D.M., Holmgren, K., Datsenko, N.M., Karlén, W., 2005. Highly variable Northern Hemisphere temperatures reconstructed from low- and high-resolution proxy data. Nature 433, 613-617.

Moros, M., Emeis, K., Risebrobakken, B., Snowball, I., Kuijpers, A., McManus, J., Jansen E., 2004. Sea surface temperatures and ice rafting in the Holocene North Atlantic: climate

influences on northern Europe and Greenland. Quaternary Science Reviews 23, 2113-2126.

Moros, M., Jensen, K.G., Kuijpers, A., 2006. Mid-to late-Holocene hydrological and climatic variability in Disko Bugt, central West Greenland. The Holocene 16, 357-367.

Nesje, A., Kvamme, M., Rye, N., Reidar, L., 1991. Holocene glacial and climate history of the Jostedalsbreen region, western Norway: evidence from lake sediments and terrestrial deposits. Quaternary Science Reviews 10, 87-114.

Nesje, A., Dahl, S.O., Andersson, C., Matthews, J., 2000. The lacustrine sedimentary sequence in Sygneskardvatnet, western Norway: a continuous, high-resolution record of the Jostedalsbreen ice cap during the Holocene. Quaternary Science Reviews 19, 1047-1065.

Nesje, A., Dahl, S.O., Thun, T., Nordli, Ø., 2008. The 'Little Ice Age' glacial expansion in western Scandinavia: summer temperature or winter precipitation? Climate Dynamics 30, 789-801.

Nesje, A., 2009. Latest Pleistocene and Holocene alpine glacier fluctuations in Scandinavia. Quaternary Science Reviews 28 (21-22), 2119-2136.

Nørgaard-Pedersen, N., Spielhagen, R.F., Erlenkeuser, H., Grootes, P.M., Heinemeier, J., Knies, J., 2003. Arctic Ocean during the Last Glacial Maximum: Atlantic and polar domains of surface water mass distribution and ice cover. Paleoceanography 18, 1063.

Olsen, A., Ninnemann, U., 2010. Large $\delta^{13}C$ Gradients in the Preindustrial North Atlantic Revealed. Science 330, 658-659.

O'Neil, J.R., Clayton, R.N., Mayeda, T.K., 1969. Oxygen isotope fractionation in divalent metal carbonates. Journal of Chemical Physics 51, 5547-5558.

Pflaumann, U., Duprat, J., Pujol, C., Labeyrie, L.D., 1996. SIMMAX: A modern analog technique to deduce Atlantic sea surface temperatures from planktonic foraminifera in deep-sea sediments. Paleoceanography 11, 15-35.

Polyakov, I.V., Alekseev, G.V., Timokhov, L.A., Bhatt, U.S., Colony, R.L., Simmons, H.L., Walsh, D., Walsh, J.E., Zahkharov, V.F., 2004. Variability of the Intermediate Atlantic Water of the Arctic Ocean over the last 100 Years. Journal of Climate 17, 4485-4497.

Polyakov, I.V., Beszczynska, A., Carmack, E.C., Dmitrenko, I.A., Fahrbach, E., Frolov, I.E., Gerdes, R., Hansen, E., Holfort, J., Ivanov, V.V., Johnson, M.A., Karcher, M., Kauker, F., Morison, J., Orvik, K.A., Schauer, U., Simmons, H.L., Skagseth, Ø., Sokolov, V.T., Steele, M., Timokhov, L.A., Walsh, D., Walsh, J.E., 2005. One more step toward a warmer Arctic. Geophysical Research Letters 32, L17605.

Quadfasel, D., Gascard, J.-C., Koltermann, K.-P., 1987. Large-Scale Oceanography in Fram Strait During the 1984 Marginal Ice Zone Experiment. Journal of Geophysical Research 92(C7), 6719-6728.

Quadfasel, D., Rudels, B., Kurz, K., 1988. Outflow of dense water from a Svalbard fjord into the Fram Strait. Deep-Sea Research 35, 1143-1150.

Rasmussen, T.L., Thomsen, E., 2009. Stable isotope signals from brines in the Barents Sea: Implications for brine formation during the last glaciation. Geology 37, 903-906.

Reimer, P.J., Baillie, M.G.L., Bard, E., Bayliss, A., Beck, J.W., Blackwell, P.G., Bronk Ramsey, C., Buck, C.E., Burr, G.S., Edwards, R.L., Friedrich, M., Grootes, P.M., Guilderson, T.P., Hajdas, I., Heaton, T.J., Hogg, A.G., Hughen, K.A., Kaiser, K.F., Kromer, B., McCormac, F.G., Manning, S.W., Reimer, R.W., Richards, D.A., Southon, J.R., Talamo, S., Turney, C.S.M., van der Plicht, J., Weyhenmeyer, C.E., 2009. IntCal09 and Marine09 Radiocarbon Age Calibration Curves, 0–50,000 Years cal BP. Radiocarbon 51, 1111-1150.

Robinson, S.G., McCave, I.N., 1994. In Orbital Forcing of Bottom-Current Enhanced Sedimentation on Feni Drift, NE Atlantic, During the Mid-Pleistocene. Paleoceanography 9, 943-972.

Rudels, B., Meyer, R., Fahrbach, E., Ivanov, V., Østerhus, S., Quadfasel, D., Schauer, U., Tverberg, V., Woodgate, R.A., 2000. Water mass distribution in Fram Strait and over the Yermak Plateau in summer 1997. Annales Geophysicae 18, 687-705.

Saloranta, T.M., Haugan, P.M., 2001. Interannual variability in the hydrography of Atlantic water northwest of Svalbard. Journal of Geophysical Research 106(C7), 13931-13943.

Saloranta, T.M., Haugan, P.M., 2004. Northward cooling and freshening of the warm core of the West Spitsbergen Current. Polar Research 23, 79-88.

Sarjeant, W.A.S., 1974. Fossil and living dinoflagellates. Academic Press, London.

Schauer, U., 1995. The release of brine-enriched shelf water from Storfjord into the Norwegian Sea. Journal of Geophysical Research 100(C8), 16015-16028.

Schauer, U., Fahrbach, E., Østerhus, S., Rohardt, G., 2004. Arctic warming through the Fram Strait: Oceanic heat transport from 3 years of measurements. Journal of Geophysical Research 109(C6), C06026.

Schlichtholz, P., Goszczko, I., 2006. Interannual variability of the Atlantic water layer in the West Spitsbergen Current at 76.5°N in summer 1991-2003. Deep-Sea Research I 53, 608-626.

Schlichtholz, P., Houssais, M.-N., 1999. An inverse modelling study in Fram Strait. Part II: water mass distribution and transports. Deep-Sea Research 46, 1137-1168.

Schmidt, G.A., Bigg, G.R., Rohling, E.J., 1999. Global Seawater Oxygen-18 Database. http://data.giss.nasa.gov/o18data/.

Seidenkrantz, M.-S., Roncaglia, L., Fischel, A., Heilmann-Clausen, C., Kuijpers, A., Moros, M., 2008. Variable North Atlantic climate seesaw patterns documented by a late Holocene marine record from Disko Bugt, West Greenland. Marine Micropaleontology 68, 66-83.

Serreze, M.C., Barrett, A., Stroeve, J.C., Kindig, D., Holland, M.M., 2009. The emergence of surface-based Arctic amplification. The Cryosphere 3, 11-19.

Shackleton, N.J., Opdyke, N.D., 1973. Oxygen Isotope and Palaeomagnetic Stratigraphy of Equatorial Pacific Core V28-238: Oxygen Isotope Temperatures and Ice Volumes on a 10^5 Year and 10^6 Year Scale. Quaternary Research 3, 39-55.

Sicre, M.-A., Jacob, J., Ezat, U., Rousse, S., Kissel, C., Yiou, P., Eiríksson, J., Knudsen, K.-L., Jansen, E., Turon, J.-L., 2008. Decadal variability of sea surface temperatures off North Iceland over the last 2000 years. Earth and Planetary Science Letters 268, 137-142.

Simstich, J., Sarthein, M., Erlenkeuser, H., 2003. Paired $\delta^{18}O$ signals of *Neogloboquadrina pachyderma* (s) and *Turborotalia quinqueloba* show thermal stratification structure in Nordic Seas. Marine Micropaleontology 48, 107-125.

Ślubowska, M.A., Koç, N., Rasmussen, T.L., Klitgaard Kristensen, D., 2005. Changes in the flow of Atlantic water into the Arctic Ocean since the last deglaciation: Evidence from the northern Svalbard continental margin, 80°N. Paleoceanography 20, PA4014.

Ślubowska-Woldengen, M., Rasmussen, T.L., Koç, N., Klitgaard Kristensen, D., Nilsen, F., Solheim, A., 2007. Advection of Atlantic Water to the western and northern Svalbard shelf since 17,500 cal yr BP. Quaternary Science Reviews 26, 463-478.

Spielhagen, R.F., Erlenkeuser, H., 1994. Stable oxygen and carbon isotopes in planktic foraminifers from Arctic Ocean surface sediments: Reflection of the low salinity surface water layer. Marine Geology 119, 227-250.

Spielhagen, R.F., Werner, K., Aagaard-Sørensen, S., Zamelczyk, K., Kandiano, E., Budeus, G., Husum, K., Marchitto, T.M., Hald, M., 2011. Enhanced modern heat transfer to the Arctic by warm Atlantic Water. Science 331, 450-453.

Stuiver, M., Reimer, P.J., 1993. Extended ^{14}C data base and revised CALIB 3.0 ^{14}C age calibration program. Radiocarbon 35(1), 215-230.

Svendsen, J.I., Mangerud, J., 1997. Holocene glacial and climatic variations on Spitsbergen, Svalbard. The Holocene 7, 45-57.

Swift, J.H., Koltermann, K.P., 1988. The Origin of Norwegian Sea Deep Water. Journal of Geophysical Research 93(C4), 3563-3569.

Tarussov, A., 1992. The Arctic from Svalbard to Severnaya Zemlya: climatic reconstructions from ice cores, in: Bradley, R.S., Jones, P.D. (Eds.), Climate since A.D. 1500. Routledge, London, New York, pp. 505-516.

Taylor, F.J.R. (Ed.), 1987. The Biology of Dinoflagellates. Botanical Monographs 21. Blackwell Scientific Publications, Oxford.

Vinje, T., 1999. Barents Sea ice edge variation over the past 400 years. Extended abstract. Workshop on Sea-Ice Charts of the Arctic, Seattle, WA. World Meteorological Organization, WMO/TD No. 949, 4-6.

Vinje, T., 2001. Anomalies and Trends of Sea-Ice Extent and Atmospheric Circulation in the Nordic Seas during the Period 1864–1998. Journal of Climate 14, 255-267.

Volkmann, R., 2000. Planktic foraminifer ecology and stable isotope geochemistry in the Arctic Ocean: implications from water column and sediment surface studies for quantitative reconstructions of oceanic parameters. Berichte zur Polarforschung 361, 1-128.

Volkmann, R., Mensch, M., 2001. Stable isotope composition ($\delta^{18}O$, $\delta^{13}C$) of living planktic foraminifers in the outer Laptev Sea and the Fram Strait. Marine Micropaleontology 42, 163-188.

Walton, P., 1952. Techniques for recognition of living foraminifera. Foraminiferal Research 3, 56-60.

Werner, A., 1993. Holocene moraine chronology, Spitsbergen, Svalbard: lichenometric evidence for multiple Neoglacial advances in the Arctic. The Holocene 3, 128-137.

Zamelczyk, K., Husum, K., Rasmussen, T., Hald, M., Werner, K., Spielhagen, R.F., in prep. Climate and surface ocean conditions during the last two millennia in the Fram Strait, Polar North Atlantic: Distribution of planktic foraminifera and shell weight.

Figure captions

Fig. 1. Map of the Norwegian-Greenland Sea with respect to the major currents and the hydrography of the Fram Strait (modified after Jakobsson et al., 2008). Also indicated is the core site MSM5/5-712-1.

Fig. 2. The salinity/$\delta^{18}O$ relationship of the water column in the eastern Fram Strait (100-500 m water depth; Frank, 1996; Meredith et al., 2001; black dots and black correlation line). Also shown is the mixing line from the nearby Kongsfjorden, Svalbard based on MacLachlan et al. (2007) (grey dashed line).

Fig. 3. (a) Age-depth model. Calendar years vs. core depth for box core MSM5/5-712-1 (Table 1, Spielhagen et al., 2011). Radiocarbon dates were converted into calendar ages using the Calib version 6.0 software (Stuiver and Reimer, 1993). Dots indicate calibrated ages with a 1σ uncertainty (white bars within black dots). (b) The sedimentation rates are indicated to the corresponding linear interpolation curves, respectively.

Fig. 4. Multiproxy data set of box core MSM5/5-712-1. Approximate time frames for North Atlantic climate events are given above. Grey and white bars mark time intervals referred to in the text (RWP: Roman Warm Period, DACP: Dark Ages Cold Period, MCA: Medieval Climate Anomaly; LIA: Little Ice Age). Black dots indicate AMS datings with 1σ uncertainty (white bars). Ranges of present-day conditions (temperature, salinity, equilibrium calcite $\delta^{18}O$) are indicated by grey dashed lines.

Fig. 5. Planktic foraminifer percentages of (a) *N. pachyderma* and (b) *T. quinqueloba* shown for different size fractions. Dashed square indicate interval with percentages of *T. quinqueloba* in size fraction 150-250 µm exceeding those in size fraction 100-250 µm. (c) Percentages of *Globigerinita* sp. (black) and *N. incompta* (grey) in size fraction 100-250 µm.

Fig. 6. A clear neoglaciation trend is marked by IRD increase (a) during the last two millennia. Planktic foraminifer flux (b) is used to indicate whether sea ice coverage (white box and arrow), ice-free (grey box and arrow) or sea ice marginal conditions (dashed box and arrow) prevailed at the site. Strong Atlantic Water inflow is correlated to percentages of subpolar vs. polar planktic foraminifers in size fraction 100-250 µm (c), and to percentages of *T. quinqueloba* in size fraction 150-250 µm (d). Heavy $\delta^{18}O$ values of *N. pachyderma* (planktic) and *C. wuellerstorfi* (epibenthic) (e) may be attributed to strengthened Atlantic Water (AW) inflow and to temperature (T) or salinity (S) changes (black arrows). Planktic and epibenthic $\delta^{13}C$ records are used to reconstruct conditions of the living habitat of planktic and benthic foraminifers (ventilation, stratification, bioproduction) in subsurface and bottom water (f). Black arrows in the SST (g) and SSS (h) records highlight certain trends of AW inflow. Summer SST and summer SSS reconstructions derived from dinocyst assemblages by Bonnet et al. (2010) are also shown (MAT: grey dashed line, ANN (based on MAT sites): grey solid line). (i) Normalized 6-year running mean of Atlantic Water temperature anomalies since 1895 (i; Polyakov et al., 2004) confirm increasing temperatures and salinities of our reconstruction (SD = standard deviation) during the past ca 100 years. Black dots indicate AMS datings with 1σ uncertainty (white bars).

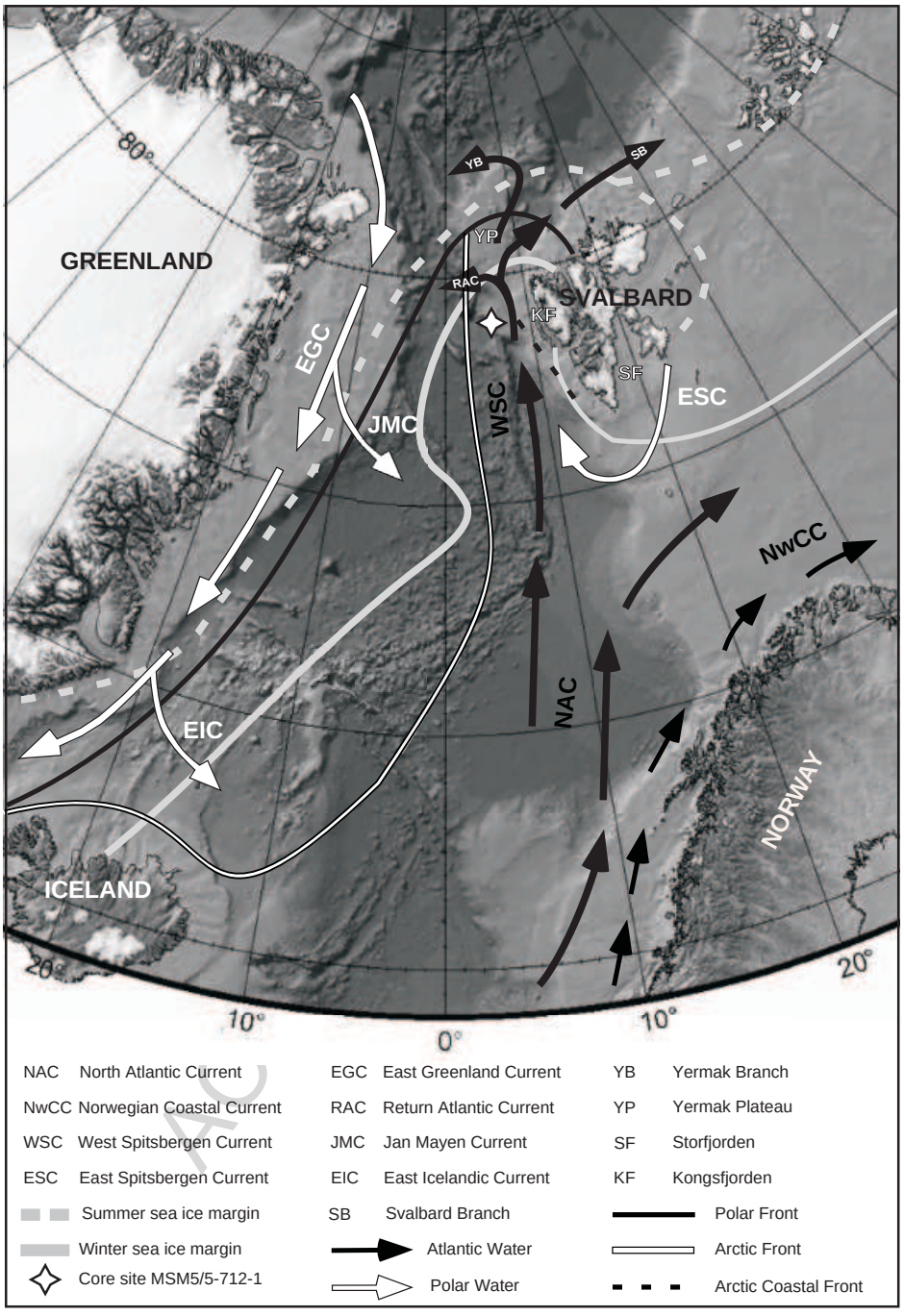

Fig. 1

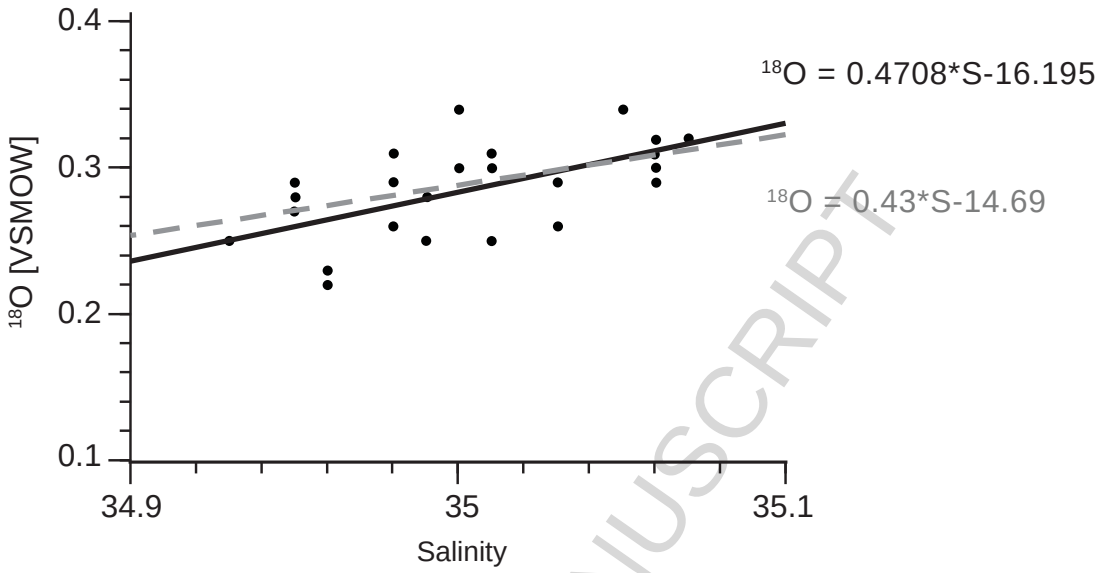

Fig. 2

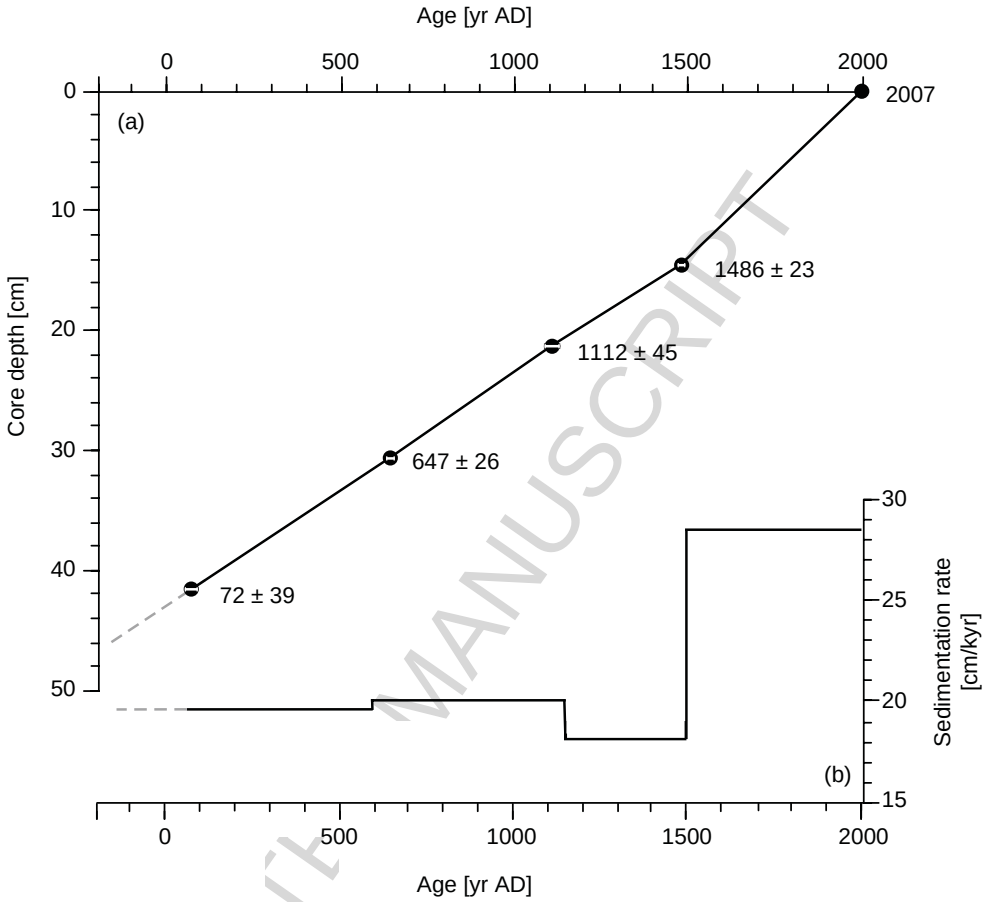

Fig. 3

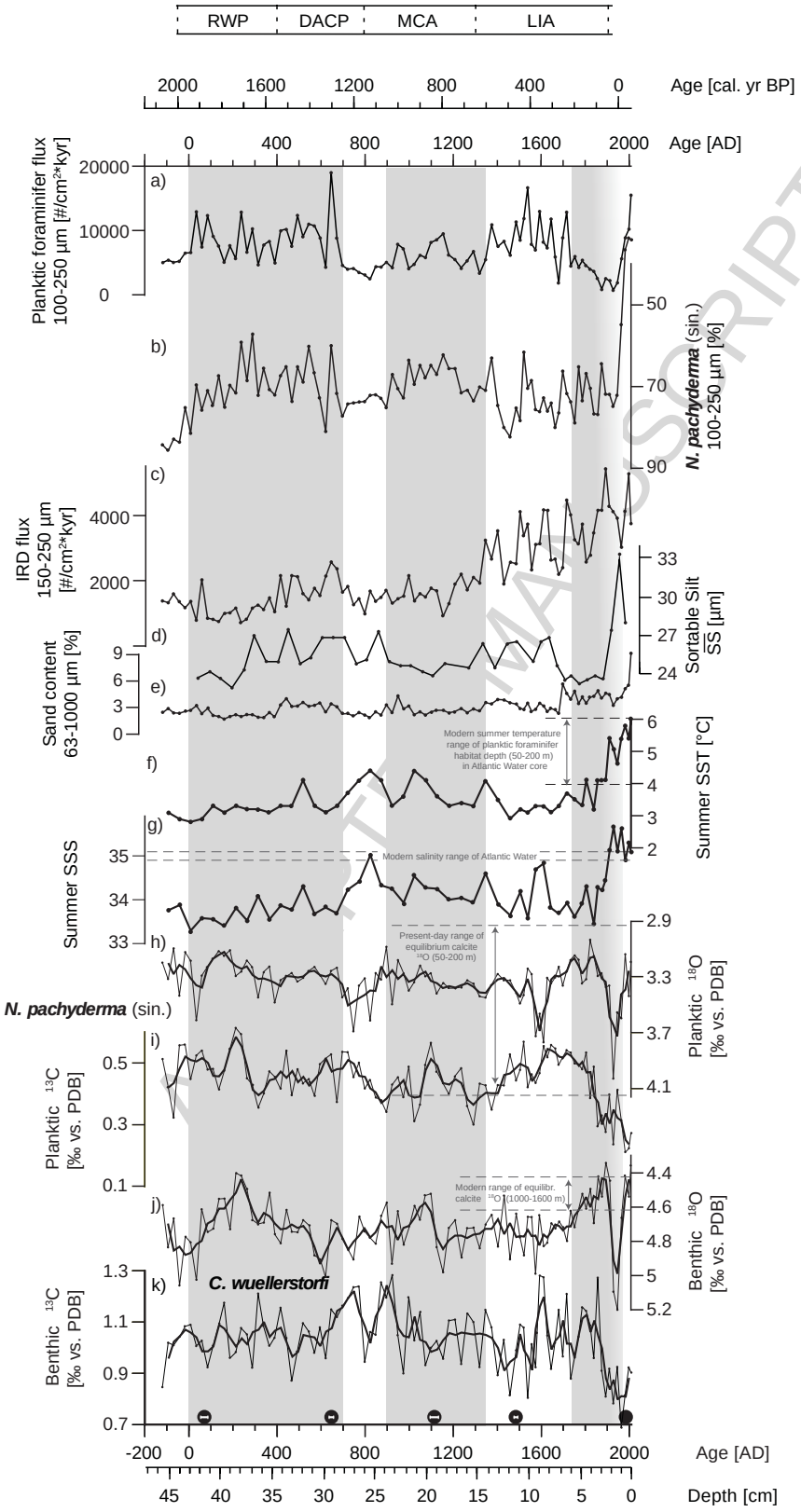

Fig. 4

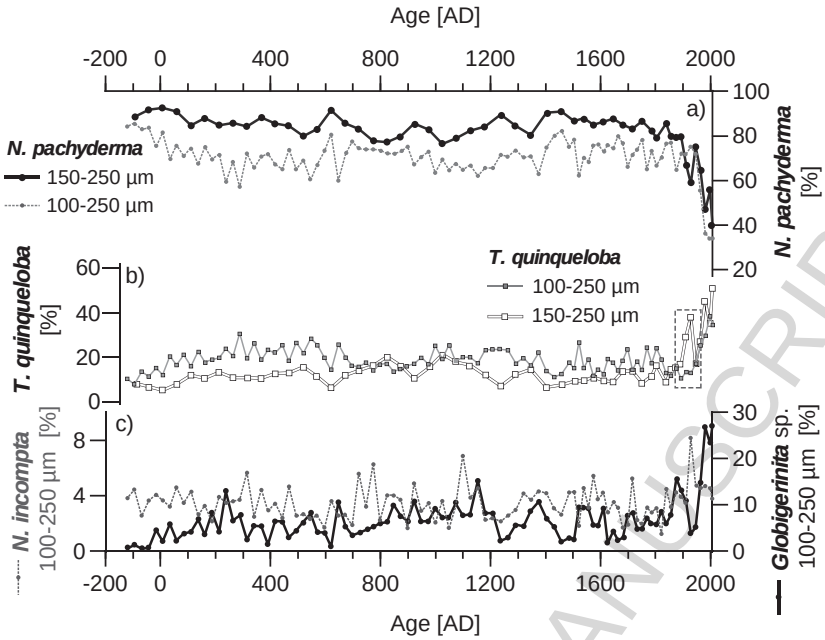

Figure 5

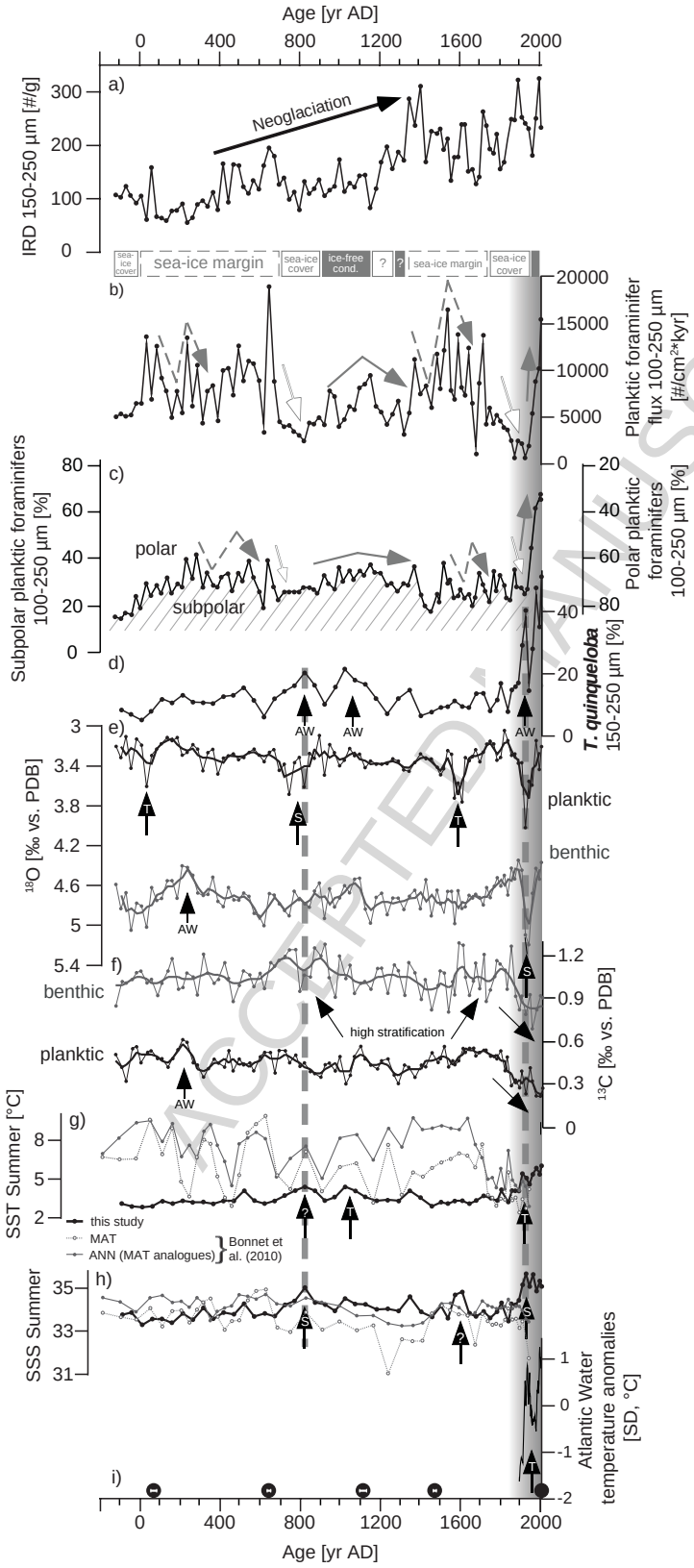

Figure 6

Table 1 AMS radiocarbon dates and calibrated dates for box core MSM5/5-712-1 (see also Spielhagen et al., 2011).

Depth, cm	Dated material	^{14}C age, yr	Cal. age, yr BP (1σ)	Cal. age, yr AD	Lab. no
0	planktic foraminifers		0	>1954 (103.47 ± 0.32 pMC corrected)	KIA 39656
14.5-15.0	*N. pachyderma*	820 ± 25	464 ± 23	1486 ± 23	KIA 39262
21.0-22.0	*N. pachyderma*	1290 ± 30	838 ± 45	1112 ± 45	KIA 39041
30.5-31.0	*N. pachyderma*	1760 ± 25	1303 ± 26	647 ± 26	KIA 39263
41.5-42.5	*N. pachyderma*	2270 ± 25	1878 ± 39	72 ± 39	KIA 38079

Research highlights

- variable conditions in the eastern Fram Strait during past 2 millennia
- varying intensity of Atlantic Water (AW) inflow affects position of sea-ice margin
- sea-ice margin fluctuated over the site between ~1 to 700 AD and ~1350 to 1730 AD
- heavy sea-ice conditions and weakened AW inflow during late Little Ice Age
- modern strength of AW inflow exceeds those of Medieval Climate Anomaly